EFFICACY ANALYSIS OF A COMPRESSED AIR OXYGENATION SYSTEM FOR AQUACULTURE ENERGIZED BY A FLOATING PV POWER GENERATION SYSTEM

SIRISAK PANGVUTHIVANICH

A DISSERTATION SUBMITTED IN PARTIAL FULLFILLMENT OF THE REQUIREMENT FOR THE DEGREE OF DOCTOR OF ENGINEERING PROGRAM IN ENERGY AND MATERIALS ENGINEERING
FACULTY OF ENGINEERING
RAJAMANGALA UNIVERSITY OF TECHNOLOGY THANYABURI
ACADEMIC YEAR 2024

EFFICACY ANALYSIS OF A COMPRESSED AIR OXYGENATION SYSTEM FOR AQUACULTURE ENERGIZED BY A FLOATING PV POWER GENERATION SYSTEM

SIRISAK PANGVUTHIVANICH

A DISSERTATION SUBMITTED IN PARTIAL FULLFILLMENT OF THE REQUIREMENT FOR THE DEGREE OF DOCTOR OF ENGINEERING PROGRAM IN ENERGY AND MATERIALS ENGINEERING
FACULTY OF ENGINEERING
RAJAMANGALA UNIVERSITY OF TECHNOLOGY THANYABURI
ACADEMIC YEAR 2024

Dissertation Title	Efficacy Analysis of a Compressed Air Oxygenation System for Aquaculture Energized by a Floating PV Power Generation System
Name-Surname	Mr. Sirisak Pangvuthivanich
Program	Energy and Materials Engineering
Dissertation Advisor	Associate Professor Wirachai Roynarin, Ph.D.
Academic Year	2024

DISSERTATION COMMITTEE

.... Chairman
(Associate Professor BoonRuang Marungsri, D.Eng.)

.... Committee
(Associate Professor Boonyang Plangklang, Dr.-Ing.)

.... Committee
(Associate Professor Teerapot Wessapan, Ph.D.)

.... Committee
(Associate Professor Kiattisak Sangpradit, Ph.D.)

.... Committee
(Associate Professor Wirachai Roynarin, Ph.D.)

Approved by the Faculty of Engineering, Rajamangala University of Technology Thanyaburi in Partial Fulfillment of the Requirements for the Degree of Doctor of Engineering

.... Dean of Faculty of Engineering
(Associate Professor Sorapong Pavasupree, Ph.D.)
26 May 2025

Dissertation Title	Efficacy Analysis of a Compressed Air Oxygenation System for Aquaculture Energized by a Floating PV Power Generation System
Name – Surname	Mr. Sirisak Pangvuthivanich
Program	Energy and Material Engineering
Dissertation Advisor	Associate Professor Wirachai Roynarin, Ph.D.
Academic Year	2024

ABSTRACT

Water purification processes contribute to atmospheric pollution and carbon emissions due to the reliance on fossil fuel-based electricity for conventional aeration equipments. To address these challenges, this study examined the integration of Floating Photovoltaic (FPV) systems to compress the air and oxygenation as a sustainable energy solution for aquaculture applications.This study showed the developed and evaluated of a novel compressed air oxygenation system for aquaculture powered by FPV .

The experiment involved developing and data monitoring recorded a prototype system for about four months at an aquaculture facility in Pathum Thani Province, Thailand. The system comprised of 3.03 kWp FPV array, 3.7 kW air compressor unit, and 150 liters of air storage tank. Solar energy generate elecricity to compress the air to the agriculture pond were examined in this study.

The results shown that the FPV system generated electroicity of about 12.5 kWh daily, maintaining dissolved oxygen levels between 5.12 and 6.47 mg/L, significantly higher than the baseline of 1.7 mg/L. This study shown the new found out that at about of 1,000 W/m² solar radiation, the system achieved compressed air production of about18 m³/hr . Additionaly, the system shown the power-to-air conversion efficiency of 6.40 m³/kWh and 45% operational efficiency.The system achieved annual energy cost savings of 32,850 THB and CO_2e emission reduction of 2,956 kg, with about 6-years payback period.

Keywords: Floating Photovoltaic (FPV), compressed air oxygenation, aquaculture, dissolved oxygen, renewable energy, photovoltaic application

Acknowledgements

The researcher would like to express sincere and profound gratitude to the Energy Research and Service Centre (ERSC), Faculty of Engineering, Rajamangala University of Technology Thanyaburi, for their generous support in providing essential testing equipment. The assistance and resources provided by the center were instrumental in ensuring the smooth and efficient execution of this research.

Furthermore, the researcher extends heartfelt thanks to FT Energy Co., Ltd. for their invaluable support in facilitating the testing site. Their generosity and collaboration played a crucial role in enabling the successful implementation of our field experiments, significantly enhancing the quality and completeness of the research outcomes.

The researcher also wishes to express deep appreciation to **Associate Professor Wirachai Roynarin**, the thesis advisor, for his invaluable guidance, expertise, and unwavering support throughout the research process. His insightful feedback and encouragement were crucial in shaping the direction and success of this study.

Secondly, the researcher would like to extend sincere gratitude to the thesis committees: Associate Professor Dr. Boonruang Marungsri from the School of Electrical Engineering, Institute of Engineering, Associate Professor Boonyang Plangklang, Associate Professor Kiattisak Sangpradit, and Associate Professor Teerapot Wessapan for their valuable comments, constructive feedback, and helpful suggestions, which greatly contributed to the refinement and improvement of this research.

Finally, the researcher would like to express heartfelt thanks to their family for their unconditional love, encouragement, and unwavering support throughout this academic journey.

Sirisak Pangvuthivanich

Table of Contents

Table of Contents (Continued)

Table of Contents (Continued)

List of Tables

List of Figures

List of Abbreviations

CAPEX	Capital Expenditure
CO_2	Carbon Dioxide
DO	Dissolved Oxygen
CO_2e	A metric used to standardize the climate impact of various greenhouse gases
F.A.D.	Free Air Discharge
FPV	Floating Photovoltaic
GHG	Greenhouse Gas
GRU	Gated Recurrent Unit
HDPE	High-Density Polyethylene
IMTA	Integrated Multi-Trophic Aquaculture
IoT	Internet of Things
kWh	Kilowatt-hour (unit of energy)
kWp	Kilowatt-peak (measure of solar panel output capacity)
L/min	Liters per minute
LSTM	Long Short-Term Memory
m^3/kWh	Cubic meters per kilowatt-hour (measure of compressed air efficiency)
MAE	Mean Absolute Error
MAPE	Mean Absolute Percentage Error
mg/L	Milligrams per liter (measure of dissolved oxygen concentration)
OPEX	Operational Expenditure

List of Abbreviations (Continued)

PID	Proportional-Integral-Derivative (control algorithm)
PSH	Peak Sun Hour
PV	Photovoltaic
RAS	Recirculating Aquaculture System
RMSE	Root Mean Square Error
RNN	Recurrent Neural Network
ROI	Return on Investment
RPM	Revolutions Per Minute
SEC	Specific Energy Consumption
THB	Thai Baht (currency)
VFD	Variable Frequency Drive
W/m^2	Watts per square meter (measure of solar irradiance)

Units & Conversions

1 Ngan	≈ 400 m^2 (Thai land measurement)
1 m^3	= 1,000 L
1 bar	≈ 100 kPa
1 hp	≈ 746 W

List of Nomenclatures

C	Actual oxygen concentration	(mg/L)
C_S	Saturation concentration of oxygen	(mg/L)
Kla	Overall mass transfer coefficient	(h^{-1})
P	Power	(W or kW)
V	Volume	(m^3 or L)
T	Temperature	(°C or K)
η	Efficiency	(%)
ρ	Density	(kg/m^3)
g	Gravitational acceleration	(9.81 m/s^2)
r	Radius	(m)
h	Height or stroke length	(m)
RPM	Revolutions per minute	
W	Work	(Joules)
P_1, P_2	Initial and final pressures	(Pa or bar)
V_1, V_2	Initial and final volumes	(m^3)

CHAPTER 1
INTRODUCTION

1.1 Background and Problem Statement

The global aquaculture industry faces mounting pressure to intensify production while maintaining environmental sustainability and economic viability. A critical challenge in this context is maintaining optimal dissolved oxygen (DO) levels, which fundamentally influence fish growth, feed conversion efficiency, and overall system productivity[1]. Traditional aeration methods, particularly grid-powered paddle wheels and surface aerators present significant limitations in energy efficiency and operational costs, especially in remote or off-grid locations.

The convergence of two technological developments, floating photovoltaic (FPV) systems, and compressed air oxygenation, presents a promising solution. FPV systems offer dual benefits: clean electricity generation and reduced water evaporation while potentially regulating algal growth through partial shading[2]. Compressed air oxygenation systems have demonstrated superior performance, achieving up to 30% higher oxygen transfer rates than surface aeration methods[3]. However, the energy-intensive nature of air compression has historically limited its widespread adoption.

The reliance on fossil fuel-based electricity for aquaculture oxygenation systems contributes to greenhouse gas emissions, creating a paradox where water purification processes simultaneously contribute to environmental degradation. This situation necessitates transitioning toward renewable energy solutions under the principle of "clean water, clean air."

1.2 Research Significance

Integrating solar-powered FPV systems with compressed air oxygenation presents several critical challenges and opportunities that warrant investigation.

1.2.1 System Optimization. There is a need to balance solar power generation capacity with compressed air system energy requirements across diurnal cycles.

1.2.2 Environmental Impact. Understanding the ecological implications of partial shading from FPV installations on pond ecosystems.

1.2.3 Economic Viability. Conducting comprehensive cost-benefit analyses comparing integrated systems with conventional aeration methods.

1.2.4 Technical Integration. Developing robust control systems to manage variable power output from solar installations.

While previous research has examined solar installations and compressed air oxygenation systems independently, limited attention has been paid to their integrated performance, particularly regarding oxygen transfer efficiency under variable solar power conditions.

1.3 Research Objectives

This study aims to

1.3.1 Evaluate and analyze engineering variables critical to aeration systems in aquaculture, with a specific focus on renewable energy integration.

1.3.2 Develop and validate a prototype compressed air system capable of demonstrably reducing greenhouse gas emissions in aquaculture operations.

1.3.3 Establish standardized specifications for compressed air systems suitable for commercial deployment.

1.4 Research Methodology

The research employs a mixed-methods approach comprising.

1.4.1 Comprehensive literature review examining relevant research, identifying advantages and limitations of existing systems, and establishing the scope of investigation.

1.4.2 Simulation analysis using PVsyst software to calculate solar energy potential and projected electrical energy production.

1.4.3 Comparative analysis of energy consumption between fossil fuel-based and solar-powered compressed air systems.

1.4.4 Engineering calculations and system design optimization.

1.5 Research Framework

The study follows a structured framework encompassing.

1.5.1 Solar potential analysis using PVsyst simulation software

1.5.2 Energy consumption calculations for compressed air production (500 L/min)

1.5.3 Air supply rate calculations and mechanical system design

1.5.4 System implementation in a test facility (1 ngan area)

1.5.5 Performance monitoring and data collection

1.5.6 Comparative analysis between actual and designed performance metrics

1.5.7 Knowledge dissemination and commercialization strategy development

1.6 Scope and Limitations

The research focuses on

1.6.1 Design and implement a solar-powered air compressor system with 500 L/min capacity for a 1-ngan natural water source.

1.6.2 Water quality parameters aligned with Department of Fisheries standards for freshwater aquaculture.

1.7 Research Assumptions

The study operates under the assumption that direct coupling of solar panels to air compressors may enable system operation under lower light conditions compared to grid-connected systems. This hypothesis will be tested through a comparative analysis of:

1.7.1 Light intensity versus compressed air production

1.7.2 Direct coupling versus grid-connected system efficiency

1.7.3 Greenhouse Gas Emission Reduction Potential

1.8 Expected Outcomes

The research anticipates delivering.

1.8.1 Comprehensive understanding of engineering variables affecting aquaculture aeration using renewable energy systems.

1.8.2 Validated prototype demonstrating measurable greenhouse gas emission reductions.

1.8.3 Standardized specifications for commercial-scale implementation.

1.9 Thesis Structure

The thesis comprises five chapters

Chapter 10 : Introduction: Research context, objectives, and framework

Chapter 2 : Literature Review: Current state of knowledge in aquaculture oxygenation and renewable energy integration

Chapter 3 : Research Methodology: Detailed experimental design and analytical procedures

Chapter 4 : Results and Discussion: Findings analysis and implications

Chapter 5 : Conclusions and Recommendations: Summary of findings and future research directions

CHAPTER 2
LITERATURE REVIEW AND BASIC THEORY

This chapter discusses the foundational concepts, theories, and research relevant to analyzing compressed air systems for oxygenation in floating solar farms. The sections include related research, solar technology, wastewater treatment and aeration systems, compressed air theory, and greenhouse gas emission calculations.

1. Related research
2. Overview of Aquaculture Systems
3. Compressed Air Oxygenation Systems in Waste water treatment
4. Renewable Energy in Aquaculture
5. Floating PV Power Generation System.
6. Integration of Compressed Air Oxygenation with Floating PV Systems.
7. Deep Learning Applications in Aquaculture Systems.
8. Calculation of Greenhouse Gas Emission Coefficient.

2.1 Related research

The intensification of aquaculture practices to meet growing global seafood demand has emphasized the critical importance of maintaining optimal dissolved oxygen (DO) levels in aquaculture systems. Managing dissolved oxygen, alongside other water quality parameters such as pH, temperature, and salinity, is fundamental to aquatic life and directly impacts system productivity[4]. Several studies have investigated the efficacy of single-point versus multi-point dissolved oxygen (DO) measurement in aquaculture systems, suggesting minimal significant differences between the two approaches under specific conditions. Conducted a comprehensive assessment of DO monitoring strategies in solar-powered aquaculture systems across three commercial fish farms, comparing single central-point measurements against distributed six-point grid monitoring[4]. Their results demonstrated that in well-mixed ponds with properly designed aeration systems, the mean deviation between single-point and multi-point measurements was only 0.32 ± 0.14 mg/L, which falls within acceptable operational parameters for most commercial aquaculture species. The researchers concluded that

While multi-point monitoring provides more comprehensive spatial data, single-point measurements offer sufficient accuracy for routine management decisions in homogeneously aerated ponds, particularly when diffusers are strategically positioned, and uniform water circulation is maintained[5]. This finding has significant implications for cost-effective monitoring solutions in sustainable aquaculture operations.[5] Dissolved oxygen (DO) monitoring technologies have evolved significantly in recent years, with optical luminescence sensors increasingly replacing traditional electrochemical methods due to their superior stability and lower maintenance requirements[6]. Modern wastewater treatment facilities employ advanced DO control strategies integrating machine learning algorithms to optimize aeration energy consumption while maintaining treatment performance[7],[8]. These intelligent control systems have demonstrated energy savings of 15-30% compared to conventional approaches[9].The integration of wireless sensor networks has enabled real-time spatial DO monitoring across treatment tanks, providing unprecedented insights into oxygen transfer patterns and microbial activity distribution [10],[11]. Recent developments in anti-fouling coatings have extended sensor calibration intervals from weeks to months, significantly reducing maintenance costs in challenging wastewater environments [12,][13]. Digital twin technologies now incorporate DO data streams to create high-fidelity process models for predictive optimization and fault detection [14],[15]. Furthermore, the emergence of multiparameter probes that simultaneously measure DO, ammonium, nitrate, and phosphate has enabled more sophisticated nutrient removal control strategies[16],[17]. Recent regulatory frameworks emphasizing energy efficiency and greenhouse gas reduction have accelerated the adoption of precision DO monitoring technologies across municipal utilities [18],[19]. The emergence of floating photovoltaic (FPV) systems, particularly in aquaculture (AquaPV), represents a promising solution for addressing energy costs and environmental sustainability. Recent studies have demonstrated that FPV installations can significantly reduce operational expenses, which constitute a major component of aquaculture production costs, thereby contributing to enhanced food security, particularly in Southeast Asia[20]. Technical evaluations of FPV systems have shown impressive capabilities, with modern installations achieving maximum voltages of 406.2 Volts under optimal conditions through series-connected solar panel configurations, each module capable of 330 Wp power output [21]. However, the performance advantages of FPV systems are highly site-specific, with energy yield differences between land-based and offshore installations varying from 20% to -4%, depending on environmental factors such as irradiation levels, ambient temperature, wind speed, precipitation, and sea surface temperature [22].

Integrating advanced monitoring and control systems has become increasingly crucial in modern aquaculture operations. Recent developments in microcontroller-based systems have demonstrated effectiveness in managing dissolved oxygen conditions with high precision, offering flexibility in programming various DO regimes while achieving accuracy comparable to existing control systems [23]. Furthermore, IoT-based monitoring systems have successfully tracked critical water quality parameters, including DO concentration, pH, and temperature, while providing automated alerts when parameters deviate from preset thresholds. These systems have been successfully implemented in practical applications, particularly in Vietnamese coastal aquaculture, demonstrating alignment with specialized meter measurements[24]. Conducted a comprehensive analysis of FSPV systems, demonstrating their capability to provide reliable electricity supply for 9-11 hours daily. A notable finding was that FSPV systems achieve a 10.04% higher energy output than traditional land-based photovoltaic installations[25]. This superior performance can be attributed to the cooling effect of water bodies and optimal space utilization, as the system occupies less than 1% of the reservoir area while maintaining minimal ecological impact. Provided valuable insights into the environmental factors affecting FSPV performance, particularly focusing on humidity and cooling effects[26]. Their research revealed several key findings. The humidity Impact significant 18% reduction in steady-state temperature (Tpv) was observed at 55% relative humidity in seashore locations, and temperature reduction led to a 4% increase in PV efficiency compared to inland installations

The evolution of aquaculture technology has witnessed significant advances through the implementation of Recirculating Aquaculture Systems (RAS), Integrated Multi-Trophic Aquaculture (IMTA), and precision aquaculture methods. These innovations, along with the integration of genetic technologies, alternative feeds, and disease prevention methods, represent a significant shift towards environmentally friendly and economically viable aquaculture practices[27]. The successful operation of these systems requires careful consideration of multiple factors, including:

1. Environmental Parameters: Temperature, salinity, dissolved oxygen, and pH maintenance within optimal ranges.
2. Operational Factors: Stocking density, feed composition, feeding frequency, and disinfection methods
3. System Design: Integration of solar power generation with aeration systems.
4. Economic Viability: Balance between installation costs and operational benefits.

While existing research has extensively documented individual components of sustainable aquaculture systems, a significant gap exists in understanding the comprehensive performance of integrated solar-powered compressed air oxygenation systems. This research deficit encompasses:

- The optimization of power management between solar generation and aeration requirements.
- The impact of variable solar output on oxygen transfer efficiency.
- The development of robust control systems for maintaining stable DO levels under fluctuating power conditions.
- The economic feasibility of integrated systems for different scales of aquaculture operations

2.2 Overview of Aquaculture Systems

Aquaculture encompasses a variety of systems designed to cultivate aquatic organisms in controlled environments. These systems vary in technology and resource intensity.

2.2.1 Pond Aquaculture: Traditional, cost-effective systems relying on natural processes but requiring extensive land use.

2.2.2 Recirculating Aquaculture Systems (RAS): Closed-loop systems offering precise water quality control with minimal water use, albeit with high operational costs.

2.2.3 Integrated Multi-Trophic Aquaculture (IMTA): Systems combining species across trophic levels to promote nutrient recycling and sustainability.

Other systems, such as biofloc technology and flow-through designs, cater to specific environmental and economic needs, demonstrating diverse approaches to aquaculture management.

2.3 Compressed Air Oxygenation Systems in Waste Water Treatment

Principles of Oxygenation

Maintaining adequate dissolved oxygen (DO) levels (optimal range: 5–9 mg/L) is crucial for aquaculture health. Temperature, salinity, and altitude affect DO levels, while mechanical systems like paddlewheels or diffused aerators enhance oxygen transfer.

Types of Oxygenation Systems.

2.3.1 Surface Aeration: Paddlewheel aerators create surface turbulence, improving gas exchange.

2.3.2 Diffused Aeration: Fine bubble diffusers offer high oxygen transfer efficiency, ideal for closed systems like RAS.

2.3.3 Pure Oxygen Injection: High-efficiency systems using pressurized chambers for oxygen saturation.

Innovations such as solar-powered aerators and biofloc integration are gaining traction, combining renewable energy with sustainable aquaculture practices. Theoretical Background: Wastewater Treatment and Aeration Systems Dissolved Oxygen Dynamics

Fundamental gas transfer principles and biological oxygen demand govern aquaculture systems' dissolved oxygen (DO) concentration. The oxygen transfer rate (OTR) in water can be expressed through the basic mass transfer equation:

$$\frac{dC}{dt} = KLa(C_S - C) \tag{2.1}$$

Where:

KLa is the overall mass transfer coefficient

C_S is the saturation concentration of oxygen

C is the actual oxygen concentration

t is time

Several environmental parameters influence the saturation concentration (CS) and can be calculated using:

$$CS = CS_0 \times \left(\frac{P}{P_0}\right) \times \exp\left(-\frac{H}{H_0}\right) \quad (2.2)$$

Where:

C_{S0} is the standard saturation concentration

P is the atmospheric pressure

P_0 is standard pressure

H is the elevation

H_0 is the scale height constant

Aeration System Mechanics

Compressed Air Systems

Compressed air oxygenation systems operate on bubble formation and gas transfer principles. The bubble size distribution significantly affects oxygen transfer efficiency. The terminal velocity (VT) of air bubbles can be expressed as:

$$VT = \sqrt{\frac{4 \times g \times r \times (\rho l - \rho b)}{3 \times C_d \times \rho}} \quad (2.3)$$

Where:

g is gravitational acceleration

d is the bubble diameter

ρl is liquid density

ρb is gas density

C_d is the drag coefficient

Paddle Wheel Aerators

The performance of paddle wheel aerators is characterized by the standard oxygen transfer rate (SOTR) and standard aeration efficiency (SAE). Emphasizes the importance of geometric design parameters in optimizing these metrics[5]. :

$$SOTR = KL_{a20} \times V \times (C_{S20} - C_0) \quad (2.4)$$

Where:

$SOTR$ = Standard Oxygen Transfer Rate (e.g., kg O2_22/h)

KL_{a20} = volumetric oxygen transfer coefficient at 20°C (h^{-1}). This term is a measure of how efficiently oxygen is transferred from the air to the water

V = volume of the water body (m^3),

C_{S20} = saturated dissolved oxygen concentration at 20°C (mg/L),

C_0 = initial dissolved oxygen concentration (mg/L).

Wastewater Treatment Processes

Biological Treatment

In recirculating aquaculture systems (RAS), biological treatment processes are fundamental to water quality management [4]. Identify critical parameters affecting treatment efficiency:

1. Nitrification Kinetics:

$$NH_{4^+} + 1.5O_2 \rightarrow NO_{2^-} + 2H^+ + H_2O \quad (2.5)$$

2. Biofilm Growth Rate:

$$\frac{dX}{dt} = \mu X - k_d X \quad (2.6)$$

Where:

$\frac{dX}{dt}$ = rate of change of biomass (biofilm) over time,

X = biofilm biomass (e.g., mass per unit area),

μ = specific growth rate from the Monod equation,

kd = detachment rate constant.

Solid Removal

The efficiency of solid removal systems is characterized by the settling velocity of particles, described by Stokes' Law :

$$vs = \frac{2}{9} \frac{(\rho p - \rho f) g d^2}{\mu} \tag{2.7}$$

Where:

vs = settling velocity of the particle (m/s),

ρp = density of the particle (kg/m³),

ρf = density of the fluid (kg/m³),

g = acceleration due to gravity (9.81 m/s²),

d = diameter of the particle (m),

μ = dynamic viscosity of the fluid (Pa·s or kg/m·s).

Control System Integration

Modern aquaculture systems employ sophisticated control mechanisms for maintaining optimal water quality[9]. demonstrates the effectiveness of microcontroller-based systems in DO management, utilizing PID control algorithms:

$$u(t) = Kp\, e(t) + Ki \int e(t)dt + Kd \frac{de(t)}{dt} \tag{2.8}$$

The integration of IoT-based monitoring systems, as described by [10], enables real-time tracking of multiple water quality parameters, including:

- Dissolved oxygen concentration
- pH levels
- Temperature
- Turbidity
- Conductivity

System Design Considerations

Environmental Parameters

The successful operation of wastewater treatment and aeration systems requires careful consideration of various environmental factors[4]. :

1. Water Quality Parameters:
   - Temperature range: 25-32°C
   - pH: 6.5-8.5
   - DO: >5 mg/L
   - Salinity tolerance ranges
2. Operational Parameters:
   - Hydraulic retention time
   - Solids retention time
   - Feeding rates and frequencies
   - Stocking densities

Energy Efficiency

The energy efficiency of aeration systems is typically measured by the Standard Aeration Efficiency (SAE):

$$SAE = \frac{SOTR}{P} \tag{2.9}$$

Where:

SAE = Standard Aeration Efficiency (e.g., kg O_2/kWh),

$SOTR$ = Standard Oxygen Transfer Rate (e.g., kg O_2/h),

P = power input to the aeration system (kW).

Advanced Treatment Technologies

Integrated Multi-Trophic Aquaculture (IMTA)

Lal et al. (2024) highlight the importance of IMTA systems in sustainable aquaculture, incorporating:

1. Nutrient Cycling:
   - Primary producers (algae)
   - Filter feeders
   - Deposit feeders

2. Water Quality Enhancement:
   - Natural biological filtration
   - Ecosystem service provision
   - Waste reduction

Emerging Technologies

Recent innovations in treatment systems include:

1. Advanced Oxidation Processes:
   - UV treatment
   - Ozonation
   - Photocatalysis
2. Membrane Technologies:
   - Ultrafiltration
   - Reverse osmosis
   - Membrane bioreactors

2.4 Renewable Energy in Aquaculture

Integrating renewable energy into aquaculture can reduce operational costs and environmental impact. Common renewable energy solutions include

2.4.1 Solar Energy: Powers aerators, pumps, and lighting, reducing grid dependency.

2.4.2 Wind Energy: Effective in coastal regions for generating power through turbines.

2.4.3 Hybrid Systems: Combining solar and wind energy ensures a stable.

2.5 Floating PV Power Generation Systems

Floating photovoltaic (FPV) systems involve installing solar panels on water surfaces, offering several advantages over ground-based PV systems.

2.5.1 Cooling Effect. The water beneath the panels helps lower their operating temperature, enhancing efficiency by approximately 5–15%.

2.5.2 Water Conservation. FPV systems reduce evaporation, helping to maintain reservoir levels.

2.5.3 Dual-Use Potential. These systems can be integrated with aquaculture, optimizing the utilization of both land and water resources.

Water cooling in FPV systems significantly improves efficiency compared to land-based PV systems. Furthermore, pontoon designs that enhance air circulation can further optimize power generation. Studies indicate that FPV systems incorporating water cooling can achieve a 5–7% increase in energy generation compared to those relying solely on air cooling. This improvement is primarily due to the superior thermal conductivity of water, which facilitates more effective heat dissipation from the photovoltaic (PV) modules, thereby lowering operating temperatures and enhancing overall system performance[28].

Environmental Impacts of FPV Systems

Water cooling in floating photovoltaic (FPV) systems significantly improves efficiency compared to land-based PV systems, with studies indicating a 5–7% increase in energy generation due to the superior thermal conductivity of water, which enhances heat dissipation and lowers operating temperatures [28]. Additionally, pontoon designs that improve air circulation can further optimize power generation. However, FPV systems can also impact water quality by altering parameters such as pH, temperature, and dissolved oxygen levels, potentially disrupting aquatic ecosystems and biodiversity [29]. On the positive side, FPV systems reduce evaporation by up to 50% when covering significant water surfaces, conserving water and enhancing hydroelectric potential [30]. Despite these benefits, concerns about ecological disruption remain, necessitating further research to fully understand the long-term impacts on aquatic habitats [30]. Mitigation strategies, such as careful site selection, water quality monitoring, and eco-friendly system designs, are essential to balance renewable energy generation with ecosystem protection [28]. Overall, FPV systems are considered promising solar energy generation technology, offering co-benefits like land and water conservation, particularly in energy-scarce regions [31],[32].

In conclusion, while FPV systems present specific environmental challenges, they also offer significant benefits, particularly regarding water conservation and renewable energy generation. Ongoing research and careful implementation are crucial to maximizing their positive impacts while minimizing potential ecological disruptions.

Solar technology

Theoretical Background: Solar Technology Integration

Solar Photovoltaic Fundamentals

The operation of floating photovoltaic (FPV) systems in aquaculture is governed by fundamental photovoltaic principles and their unique aquatic application characteristics. The power output (P) of a solar module is theoretically described by:

$$P = \eta \times A \times G \times [1 - \beta(T - TSTC)] \quad (2.10)$$

Where:

- η represents the module efficiency
- A is the active surface area
- G denotes solar irradiance
- β is the temperature coefficient
- T is the operating temperature
- $TSTC$ is the standard test condition temperature (25°C)

In practical applications, floating solar modules have demonstrated specific operational parameters, with individual modules achieving power capacities of 330 Wp, maximum voltage (Vmax) of 42 Volts, and maximum current (Imax) of 7.85 Amperes under optimal conditions[16]. The series configuration of multiple modules, typically arranged in arrays of 10 panels, can produce cumulative voltages reaching 406.2 Volts during peak solar hours.

Environmental Interaction Effects

The performance of FPV systems is significantly influenced by environmental factors, with energy yield variations between land-based and offshore installations ranging from +20% to -4% depending on site-specific conditions [33]. Key environmental parameters affecting system performance include:

1. Thermal Effects:
    - Water-cooling effect on panel temperature
    - Ambient temperature influence on conversion efficiency
    - Surface water temperature variations

2. Atmospheric Conditions:
    - Solar irradiation levels
    - Wind speed and direction
    - Precipitation patterns
    - Humidity effects
3. Water Body Characteristics:
    - Wave action and system stability
    - Water surface reflectivity
    - Aquatic ecosystem interactions

Power Management and Storage

Integrating FPV systems with aquaculture operations requires careful consideration of power management strategies. Typically configured with 12 Volt 200 Ah specifications, current battery storage systems demonstrate specific operational limitations. For example, a four-battery configuration provides approximately 12 hours of operation for limited loads, while expanded systems requiring 12 batteries may be necessary for full operational capacity[30]. The theoretical storage capacity (E) can be calculated as:

$$E = V \times I \times t \times DoD \times \eta \tag{2.11}$$

Where:

V is the nominal voltage

I is the current capacity in ampere-hours

t is the time duration

DoD is the depth of discharge

η represents system efficiency

Control Systems Integration

Modern FPV systems in aquaculture incorporate sophisticated control mechanisms for optimal operation. Microcontroller-based systems have effectively managed dissolved oxygen levels through precise control algorithms[3]. The control system architecture typically follows a proportional-integral-derivative (PID) control model:

$$u(t) = Kp\,e(t) + Ki \int e(t)dt + Kd\,\frac{de(t)}{dt} \quad (2.12)$$

Where:

$u(t)$ is the control signal

$e(t)$ is the error signal

Kp, Ki, and Kd are the proportional, integral, and derivative gains, respectively.

System Optimization Considerations

The optimization of FPV systems in aquaculture requires balancing multiple operational parameters:

1. Energy Generation Optimization:
   - Panel tilt angle optimization
   - Array configuration efficiency
   - Tracking system implementation feasibility
2. Storage System Design:
   - Battery capacity optimization
   - Charge/discharge cycle management
   - System redundancy requirements
3. Load Management:
   - Peak load handling
   - Demand response strategies
   - Emergency power provisions

Economic Framework

The economic viability of FPV systems in aquaculture is assessed through a comprehensive cost-benefit analysis, incorporating:

1. Capital Expenditure (CAPEX):
   - Solar panel array costs
   - Floating structure expenses
   - Installation and commissioning
2. Operational Expenditure (OPEX):
   - Maintenance requirements
   - System monitoring costs
   - Replacement schedules
3. Return on Investment (ROI) Factors:
   - Energy cost savings
   - Production efficiency improvements
   - Environmental benefit valuations

The implementation of FPV systems has shown potential for significantly reducing operational costs, particularly in Southeast Asian aquaculture operations[34]. However, successful deployment requires careful consideration of public engagement and policy frameworks to address ecological concerns and ensure sustainable implementation. Floating Photovoltaic (FPV) systems have the potential to achieve higher efficiency than traditional ground-mounted solar panels and conventional energy systems due to several key advantages. Firstly, FPV systems benefit from improved cooling as water absorbs and dissipates heat more effectively, enhancing photovoltaic conversion efficiency. Secondly, reduced reflection losses on water surfaces allow for greater sunlight absorption. Thirdly, minimized shading in open water bodies ensures consistent energy production. Additionally, FPV systems optimize land use by utilizing water surfaces, avoiding land-use conflicts. They also reduce water evaporation, conserving resources and maintaining water levels. Furthermore, FPV systems can inhibit algal growth, improve water quality, and support healthier aquatic ecosystems. These combined benefits make FPV a highly efficient and sustainable energy solution.

2.6 Integration of Compressed Air Oxygenation with Floating PV Systems

System Design and Integration

Integrating compressed air oxygenation with FPV involves designing an energy-efficient air compression system powered by solar energy. Essential components include PV modules, air compressors, and oxygen diffusers.

2.6.1 Compressed air theory Design of mechanical system, power transmission system, suitable gear ratio, rotational ratio per minute for motor and piston type air compressor Finding the air flow rate.

Compressed air theory

The compression process in aquaculture aeration systems follows fundamental thermodynamic principles. The work required for isothermal compression is expressed as:

$$W = P_1 V_1 ln(\frac{P_2}{P_1}) \tag{2.13}$$

Where:

W = work done by the gas (Joules),

P_1 = initial pressure of the gas (Pa),

P_2 = final pressure of the gas (Pa).

V_1 = initial volume of the gas (m³),

For adiabatic compression:

$$P_1 V_1^{k} = P_2 V_2^{k} \tag{2.14}$$

Where:

$k\ (gamma)$ = adiabatic index or specific heat ratio, defined as $k = \frac{C_V}{Cp}$

Cp = specific heat capacity at constant pressure,

Cv = specific heat capacity at constant volume.

V_1, V_2 = initial and final volumes of the gas (m³),

$P1, P2$ = initial and final pressures of the gas (Pa), Oxygen Transfer Mechanisms

Dissolved Oxygen Control

Following Mucha (2024), the control system implements PID logic:

$$u(t) = Kp \times e(t) + Ki \times \int e(t)dt + Kd \times \frac{de(t)}{dt} \tag{2.15}$$

Where:

$u(t)$ is control output

$e(t)$ is error signal

Kp, Ki, Kd are control parameters

Design of mechanical system, power transmission system, suitable gear ratio, and rotational ratio per minute for motor and piston air compressor finding the air flow rate.

Equations :

Operation of the air compressor: The amount of air obtained from the compression single-stage compression pump, 2 cylinders, diameter 95 millimeters, stroke length 85 millimeters, and efficiency 85 percent.

Calculate the amount of air per cycle. $= \frac{545\, l}{1\, min} \times \frac{1\, min}{620\, rev}$

$$= 0.879 \ \ l/rev$$

Calculate the torque of a 5 hp air compressor operating at 620 rpm.

$$P = T\omega \tag{2.16}$$

$$5 \times 746 = T\left(\frac{2\pi(620)}{60}\right)$$

$$T = 57.482\, N \cdot m$$

Calculate the torque obtained. Find the duty cycle of a 3 hp. motor.

$$P = T\omega$$

$$3 \times 746 = 57.482\left(\frac{2\pi(620)}{60}\right)$$

$$N = 248.99\, rpm$$

Find the revolution ratio of the motor. A motor operating at 1400 rpm requires an operating speed of 248.99 rpm.

$$Ratio = \left(\frac{RPM(motor)}{N}\right) \quad (2.17)$$

$$Ratio = \left(\frac{1,400}{248.99}\right)$$

$$Ratio = 5.62$$

Choose a reduction gear with a ratio of 1:5

The motor runs at 1400 rpm through a reduction gear with a 1:5 to 280 rpm ratio.

Find the volume of air produced per year when the air volume per cycle is 0.879 liters per cycle. Set the air compressor to work 8 hours a day.

Compressed air volume/hour = 0.879 liters per cycle x number of cycles x 60 minutes

= 0.879 liters per revolution x 80 rpm x 60 minutes

= 14,767 liters per hour

Compressed air volume/year = Compressed air volume/hour x 9 hours x 365 days

= 14,767 liters per hour x 9 hours x 365 days

= 48,510,000 liters per year or 48,510 cubic meters per year

Calculate the electricity cost of a 3 HP motor. (The motor consumes 4.92 amps and uses 380 volts, 3 phases.)

$$P = \sqrt{3}\,VI \times PF \times Eff. \quad (2.18)$$

$$P = \sqrt{3} \times 4.92(380) \times 0.82 \times 0.83$$

$$P = 2,203.95\,W$$

Find the electrical unit that is used/day. When the motor works 8 hours a day

$$kWh = \frac{P \times hr}{1000} \quad (2.19)$$

$$kWh = \frac{2,203.95 \times 8}{1,000}$$

$$kWh = 17.63\,kwh$$

Electricity is charged at 6 baht per unit.

$$Electricity\ cost\ =\ Electricity\ unit\ x\ Electricity\ price\ per\ unit$$

$$Electricity\ cost\ =\ 17.63\ kWh\ x\ 6\ THB$$

$$Electricity\ cost\ =\ 105.78\ \ THB/Day\quad or\ 38{,}610\ \ THB/Year$$

2.7 Deep Learning Applications in Aquaculture Systems

Integrating deep learning in aquaculture has significantly improved water quality monitoring, dissolved oxygen prediction, and system optimization. Advanced machine learning models, particularly deep neural networks, are increasingly used to enhance the efficiency of compressed air oxygenation systems in floating PV-powered aquaculture.

2.7.1 Overview of Deep Learning

Deep learning is a subset of machine learning that utilizes multi-layered artificial neural networks to analyze complex patterns in data. Common architectures include:

2.7.1.1 Convolutional Neural Networks (CNNs): Primarily used for image-based monitoring in aquaculture, such as fish health assessment.

2.7.1.2 Recurrent Neural Networks (RNNs) and Long Short-Term Memory (LSTM) Networks: Ideal for time-series predictions, including dissolved oxygen fluctuations and power demand forecasting.

2.7.1.3 Transformer Models: Emerging in predictive analytics for water quality monitoring and autonomous system control.

2.7.2 LSTM Networks for Oxygenation System Control

LSTM networks are widely used in time-series prediction because they capture long-term dependencies. LSTMs can predict dissolved oxygen levels in aquaculture based on historical sensor data, adjusting compressed air flow rates dynamically to optimize aeration efficiency. By training LSTM networks on historical data from dissolved oxygen sensors and compressed air systems, aquaculture facilities can predict oxygenation requirements and optimize energy usage from floating PV systems.

2.7.3 Applications of Deep Learning in Aquaculture

Deep learning applications in aquaculture and floating solar systems focus on three main areas: water quality prediction (including DO levels, temperature, and pH monitoring), system optimization (covering solar power generation forecasting and aeration efficiency), and fault detection (encompassing equipment maintenance and anomaly detection). These applications enable proactive system management and improved operational efficiency through predictive capabilities.

The implementation of deep learning systems requires careful consideration of three critical factors: data quality and quantity (ensuring proper sensor calibration and data preprocessing), model architecture design (including appropriate network topology and hyperparameter optimization), and system integration aspects (focusing on real-time processing capabilities and communication protocols). These considerations are essential for developing reliable, effective deep-learning solutions in aquaculture environments.

Integrating deep learning with IoT-based monitoring systems has shown promising results in practical applications. For example, predictive models have demonstrated accuracy rates exceeding 90% in forecasting DO levels 24 hours in advance, enabling proactive management of aeration systems[10].

Deep learning technology is revolutionizing modern aquaculture systems through innovative applications that enhance efficiency, sustainability, and productivity[35]. Computer vision systems utilizing convolutional neural networks now enable real-time fish health monitoring, detecting diseases before they spread throughout farming operations[36],[37]. Recurrent neural networks and transformer architectures have demonstrated remarkable accuracy in predicting water quality fluctuations, optimizing feeding schedules, and forecasting growth rates in diverse aquatic species[38],[39].Transfer learning approaches have proven valuable in adapting pre-trained models to species-specific applications with minimal additional data requirements [40],[41]. Deep reinforcement learning systems now automate critical farm management decisions, including optimal harvesting times and resource allocation strategies [42],[43]. Edge computing implementations bring these sophisticated algorithms directly to remote aquaculture facilities, enabling real-time decision support even in bandwidth-limited environments[44],[45]. Multimodal deep learning approaches combining visual, chemical, and acoustic sensor data provide previously impossible monitoring capabilities with traditional methods[46],[47]. Despite these advances, challenges remain in building robust models that generalize across the diverse environmental conditions and species variations inherent to global aquaculture operations [48].

2.7.4 Future Prospects

Integrating deep learning with Internet of Things (IoT) sensors, edge computing, and real-time control systems will further enhance aquaculture automation. Hybrid models combining LSTMs and reinforcement learning can enable autonomous decision-making, optimizing aeration and power management based on environmental conditions.

Deep learning will ensure sustainability, cost-efficiency, and precision control in aquaculture operations as floating PV-powered compressed air oxygenation systems advance.

2.8 Calculation of Greenhouse Gas Emission Coefficient

Greenhouse gas (GHG) emissions from electricity generation are calculated using certified methodologies, such as the Tool to calculate the emission factor for an electricity system[49]. Emission reductions are quantified to assess the environmental benefits of renewable energy-powered systems.

To calculate the Greenhouse Gas (GHG) Emission Coefficient from fossil fuels per kWh, you can use the following general approach.

Table 2.1 Approximate emission coefficients (values may vary based on fuel quality and power plant efficiency)

Fuel Type	Emission Factor (kg CO_2 eq/kWh)
Coal (bituminous)	0.9–1.1
Natural Gas	0.4–0.5
Oil	0.7–0.9
Solar PV	0.05-.01
Wind Energy	0.02-0.05

Impact on Aquaculture Operations

Integrating solar PV-powered compressed air oxygenation systems significantly reduces the carbon footprint of aquaculture. For example, a traditional aeration system consuming 10,000 kWh annually using grid electricity from a coal-based power plant (EF = 1.0 kg CO_2 eq/kWh) would emit approximately 10,000 kg CO_2 eq annually. Switching to a solar PV system with an emission factor of 0.05 kg CO_2 eq/kWh would reduce emissions to just 500 kg CO_2 eq.

Future Developments

Further research is needed to evaluate renewable-powered aquaculture systems' full life cycle emissions: hybrid renewable energy solutions, e.i. Combined floating PV with wind energy can minimize environmental impacts while ensuring reliability (IEA, 2021).

By integrating deep learning models with real-time energy monitoring, aquaculture facilities can optimize their aeration systems while minimizing emissions, ensuring sustainability in future aquaculture practices.

Recent research has significantly advanced our understanding of greenhouse gas emissions in integrated aquaculture-solar systems[50]. Developed a comprehensive life cycle assessment framework that considers both direct and indirect emissions from system operations, while[51],demonstrated through global case studies that floating PV integration can achieve 45-60% emission reductions compared to conventional grid-powered aquaculture systems[52]. provided valuable insights into seasonal variations of GHG emissions in Southeast Asian facilities, highlighting the importance of accounting for temporal factors in emission calculations. Additionally,[53] proposed a detailed methodology for calculating carbon payback periods in floating solar PV systems, considering embodied carbon in system components and establishing practical guidelines for assessing the long-term environmental benefits of these integrated systems.

Calculate CO_2 emissions from electricity consumption[54].

The basic equation to calculate CO_2 emissions from electricity consumption is:

$$CO^2\ Emission\ (kg) = Electricity\ Consumption\ (kWh) \times Emission\ Factor\ (kg\ CO_2/kWh) \qquad (2.20)$$

Where:

CO_2 *Emissions* are typically measured in kg CO_2 or metric tons CO_2

Electricity Consumption is measured in kilowatt-hours (kWh) or megawatt-hours (MWh)

Emission Factor is measured in kg CO_2/kWh or metric tons CO_2/MWh

CHAPTER 3
RESEARCH METHODS

This chapter outlines the methodologies used to evaluate the performance and feasibility of a compressed air oxygenation system for aquaculture powered by a floating photovoltaic (FPV) system. The study integrates experimental setup, field data collection, and computational analysis to assess the system's technical performance, energy efficiency, and environmental impact.

1. Study Area and Experimental Setup
2. Research Objectives and Hypotheses
3. Equipment and Instrumentation
4. System Design and Operation
5. Data Collection Methods
6. Data Analysis.
7. System Architecture.

3.1 Study Area and Experimental Setup

The experimental setup and measurements were conducted at Klong 4 District, Pathum Thani Province, for 4 months, encompassing variations in weather conditions, solar irradiance levels, and aquaculture operational requirements. This approach enables a thorough understanding of the system's performance across different scenarios and operational conditions. This scholarly investigation aims to meticulously analyze and develop a sophisticated prototype for a water treatment system utilizing compressed air tailored to enhance aquaculture practices. Such a system is deemed particularly appropriate given the substantial volume of water that necessitates treatment within a pond that measures approximately 1 Ngan in its width and length dimensions, combined with a depth that reaches around 3 meters, thereby indicating a considerable volumetric capacity. To effectively model the water that requires treatment for the oxygen control experiment, we will employ fish densities that reflect the established norms in fish culture, particularly in scenarios where freshwater fish are introduced into the aquatic environment. The total volume of the water within this pond is estimated to be 1,200 cubic meters, a substantial amount that facilitates the regulation of oxygen levels, essential for promoting optimal growth conditions for the fish population. Additionally, the design will incorporate a remote control mechanism capable of automatically deactivating the system whenever the oxygen concentration either exceeds or drops below a predetermined threshold, thus ensuring the maintenance of a stable aquatic ecosystem.

Figure 3.1 The 3-kW Compressed Air Oxygenation System integrates a floating PV power generation system for aquaculture uses. The location is Klong 4 District, Pathum Thani Province, Thailand.

3.2 Research Objectives and Hypotheses

Research Objectives

3.2.1 To evaluate the performance of the compressed air oxygenation system under varying solar irradiance conditions.

3.2.2 To assess energy utilization efficiency and greenhouse gas (GHG) reduction.

3.2.3 To analyze the system's economic feasibility and scalability for commercial aquaculture.

Hypotheses.

3.2.4 The air compressor system will operate effectively with low solar irradiance, initiating oxygenation at the onset of sunlight.

3.2.5 The compressed air system will demonstrate significant energy savings and reduced GHG emissions compared to conventional energy sources.

3.2.6 The floating PV-powered oxygenation system will meet aquaculture oxygenation demands under diverse operational conditions.

The air compressor system that will be used to add oxygen to this aquaculture farm will be designed to use energy from floating solar panels that are drinking water-grade plastic so as not to damage the environment. It can be used in all types of water-resistant compounds that are not easily destroyed by ultraviolet radiation and to make a buoy that will hold the solar panel. The monocrystalline type is a solar panel that does not contain cadmium that can cause harm to water and contaminants because it is made from quartz or glass sand, with the power of the solar panel size of not less than 3 kilowatt comes through a constant frequency control system with a modern control system to protect the new motor from changing the frequency and intensity of sunlight that varies according to the hours of sunshine. The control system stops power to the compressed air motor when the oxygen supply is sufficient. However, air will be compressed into the energy storage system, both the air compressor tank and the battery, which will be used to control the valve opening and closing system electrically, as well as the remote control signal transmission system and display camera. The airflow measurement system will record the value in the operation data acquisition set. To know the amount of compressed air to be stored for use in an urgent emergency when the oxygen value may not be enough during the night when there is no sun. or when the sun is less during the day to send a signal to the system to release compressed air from the compressed air tank to help add oxygen to the water treatment system in the pond in time.

Mechanical system design, power transmission system, and gear ratio suitable. Furthermore, the rotation ratio per minute for motor and piston-type air compressors is durable and produces flow and pressure that can be compressed into an air compressor as an energy storage system. The right air compresses energy storage in the reciprocating air compressor system and the right size motor and control system are essential to keep the equipment running efficiently, at low cost, and with low maintenance. It is a mechanical design suitable for the electrical power produced during each period of system operation. What is important in this research is to measure the efficiency of the compressed air system to see how many liters of compressed air per minute each day at different light intensities the system can generate on average and can compensate for the electricity consumption. Moreover, it reduces greenhouse gas emissions by determining how much the system has a break-even point in how many years of operation it has and how much it reduces human labor in aquaculture control. This design study will create a prototype to test the actual use in the aquaculture area to develop the commercially available system. Reduce technology imports and have affordable prices for farmers who want to continue using clean energy systems for aquaculture.

In general, the operation of solar cells to generate electricity has a limitation on electricity production; namely, the intensity of the amount of sunlight must be high enough for the solar cell to produce voltage until it can be connected to the power transmission system (grid). This is usually based on an estimated 5 hours per day that the solar cells can generate electricity. However, since the compressed air system in this study is used to supply electricity to the air compressor directly, the researcher hypothesized that the air compressor would be able to start when there was weak sunlight. Solar cells have started generating electricity since the beginning of sunlight, and when the air compressor can take off, It will start producing compressed air to oxygenate the water. The researcher, therefore, will conduct a test by measuring the amount of sunlight intensity compared to the amount of compressed air produced by the system, then calculate and compare with the electricity generation to supply to the power supply system first and then be supplied to the compressed air system to see what are the differences in terms of the number of units of electricity produced. The amount of air produced by the system and reduced greenhouse gas emissions from using compressed air for oxygen filling by floating solar energy.

3.3 Equipment and Instrumentation

3.3.1 Dissolved Oxygen Analyzer & Sensor

The DO analyzer measures oxygen concentration (mg/L) in the water, providing real-time data essential for maintaining optimal aquaculture conditions. The dissolved Oxygen Analyzer is shown in Figure 3.2.

Figure 3.2 Dissolved Oxygen Analyzer[56].

3.3.2 Thermal Mass Gas Flow Meter

This device measures the mass flow rate of compressed air, helping assess system efficiency and airflow distribution. Thermal Mass Gas Flow Meter shown in Figure 3.3

Figure 3.3 Thermal Mass Gas Flow Meter[57].

Thermal Mass Gas Flow meters are available in inline flow bodies or insertion styles. Either way, the meter's probe inserts into a pipe, stack, or duct gas stream. Toward the tip of the meter's probe are two sensors: resistance temperature detectors (RTDs) or resistance thermometers that measure temperature. The RTDs are durable reference-grade platinum windings clad in a protective 316 SS or Hastelloy C sheath. Thermal Mass Gas Flow Meter circuitry continuously overheats between the flow and reference detectors. An integrated circuit and functions heat one RTD as the flow sensor, while a second RTD acts as the reference sensor and determines the gas temperature. As gas flows by the heated RTD, drifting gas molecules transport heat away from it, and as a result, the sensor cools, and the energy escapes. Thermal mass flow meters function based on the principle of thermal dispersion, which leverages the variance in heat transfer rates between a thermally stimulated sensor and the fluid traversing its surface. The apparatus comprises two temperature measurement devices: one that is actively heated, while the other is equipped with a temperature compensation mechanism. As the fluid navigates over the heated sensor, it assimilates heat, resulting in a temperature differential between the two sensors. By quantifying this temperature differential, the thermal mass flow meter can precisely determine the fluid's mass flow rate (Thermal Mass Flow Meter, 2025). [56] The thermal Mass Gas Flow Meter principle is shown in Figure 3.4

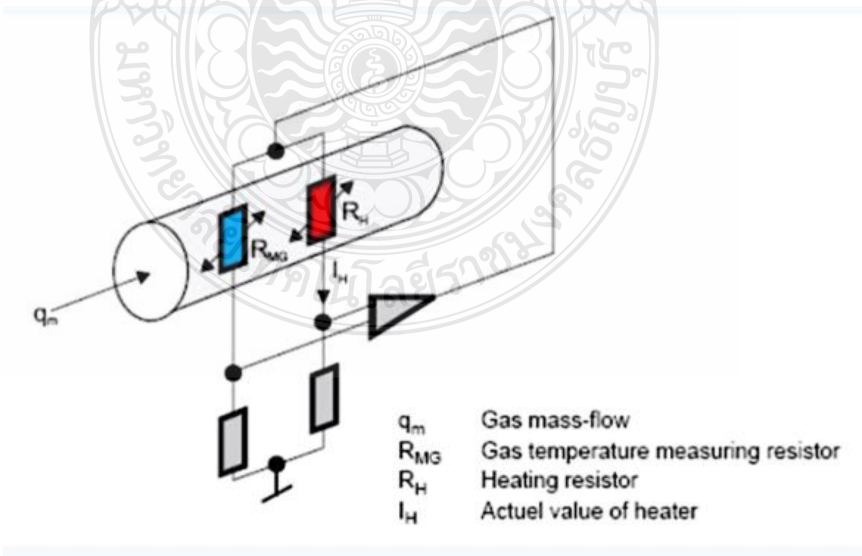

Figure 3.4 Thermal Mass Gas Flow Meter principle [57].

3.3.3 Pyranometer

Used to monitor solar irradiance, the pyranometer ensures accurate measurement of sunlight intensity at different times of the day. To analyze the intensity of sunlight compared to the performance of compressed air systems. The operational principle of the pyranometer is fundamentally predicated on the differential temperature measurement between two contrasting surfaces, namely dark and clear. The absorption of solar radiation occurs predominantly at the black surface of the thermopile, while the clear surface reflects it, resulting in diminished heat absorption.

The thermopile is integral to the assessment of the temperature differential. The potential difference generated within the thermopile arises from the thermal gradient between the two surfaces. These measurements quantify the total solar radiation incident upon the device.

However, the voltage produced by the thermopile is determined by utilizing a potentiometer for accurate assessment. Additionally, the quantification of radiation must be incorporated through methodologies such as planimetry or the utilization of an electronic integrator. (Elprocus, 2025) [57]. The pyranometer shown in Figure 3.5

Figure 3.5 Pyranometer [58].

3.3.4 Paperless Recorder

The Yokogawa GP10 paperless recorder logs multiple parameters, such as solar radiation, DO levels, and power output, at set intervals for subsequent analysis—the Paperless Recorder is shown in Figure 3.6.

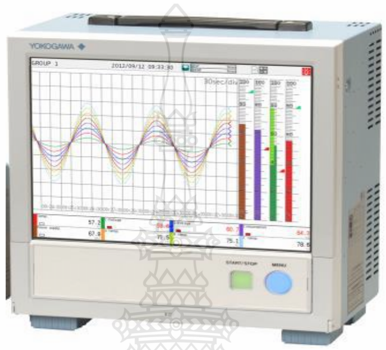

Figure 3.6 Paperless Recorder [59].

3.3.5 Power Meter

Digital power meters are used in the electronics and mechatronics fields to measure the power consumption of home appliances, office equipment, industrial machines, hybrid/electric vehicles and other battery-driven equipment, solar power/wind power generation related devices, and so on, and are helpful in product development, performance testing, and quality control. With the growing awareness of the need to save energy, protect the environment, prevent power shortages, and the like, products must be designed to save energy. Product development and manufacturing divisions must improve operational efficiency to release products quickly and with excellent power performance. Toward this end, they need power meters with high measurement efficiency.

Power meters monitor electrical parameters, including voltage, current, and power output, to evaluate the performance of the FPV system. The power Meter is shown in Figure 3.7.

Figure 3.7 Power Meter [60]

3.4 System Design and Operation

3.4.1 Floating PV system

The FPV system comprises six monocrystalline solar panels (505 W each) mounted on a high-density polyethylene (HDPE) floating platform. The platform design minimizes water surface coverage while maximizing panel efficiency., yielding a total installed capacity of 3.03 kWp. The array is mounted on a high-density polyethylene (HDPE) floating platform with a total surface area of 8 m². The platform's buoyancy system is engineered to maintain optimal panel orientation while ensuring stable operation under varying weather conditions. This configuration maximizes energy yield while minimizing water surface coverage, allowing efficient integration with aquaculture operations.

3.4.2 Compressed air oxygenation system

The air compressor operates at 620 RPM, delivering a free air discharge (F.A.D.) rate of 545 L/min. A 155-liter air storage tank ensures consistent oxygen delivery during periods of low solar irradiance. Structures 50 cm above the pond bottom, stone diffusers facilitate uniform oxygen distribution.

The compressed air oxygenation system employs an SVU(P)-205 model compressor with a rated power of 3.7 kW (5 hp), operating at 620 RPM. The unit delivers a free air discharge (F.A.D.) rate of 545 L/min, supported by a 155-liter storage tank capacity. This configuration is engineered to provide consistent air delivery for the oxygenation system in aquaculture applications. The air distribution consists of a 1-inch (25.4 mm) high-density polyethylene (HDPE) main supply line, selected for its chemical resistance and durability in aquaculture environments. The system incorporates six strategically positioned stone diffusers for optimal oxygen transfer efficiency. Each diffuser is elevated 50 centimeters from the pond bottom to maximize the oxygen dissolution path length and ensure uniform aeration distribution throughout the water column. This configuration facilitates efficient gas transfer while minimizing sediment disturbance.

3.4.3 Data Acquisition and Monitoring

A centralized GP10 data logger records parameters, including.

- Solar radiation (W/m^2) using a pyranometer.
- Electrical output from the PV system.
- Compressed air flow rate and DO levels in the pond.

The system automatically regulates oxygenation, activating or deactivating the air compressor based on DO thresholds.

The monitoring system employs a GP10 YOKOGAWA data acquisition unit for comprehensive parameter logging at 5-minute intervals. Solar radiation is measured using a pyranometer (W/m^2), while the FPV system performance is monitored through input power measurements from the solar array and corresponding inverter output power. The compressed air system's flow rate is continuously tracked to assess oxygenation efficiency. Dissolved oxygen (DO) concentrations are measured using optical DO sensors with a measurement range of 0-20 mg/L (±0.1 mg/L accuracy). All parameters are simultaneously recorded and stored in the GP10 data logger, enabling integrated analysis of system performance and environmental conditions.

Study the technical data of solar panels, buoyancy, and operation of inverters and air compressors, then create working diagrams. Study the data that must be collected for comparison analysis. After that, prepare the necessary tools for the system.

3.5 Data Collection Methods

Data Collection Methods for FPVS-Powered Compressed Air Oxygenation System Study.

3.5.1 Solar PV System Performance

Solar Irradiance Measurement

The equipment used in this study includes a pyranometer to measure solar irradiance. The primary parameters monitored are the global horizontal irradiance (W/m^2) and the array irradiance (W/m^2) plane. Data collection is conducted at a sampling interval of five minutes, ensuring high-resolution measurements. The system operates with continuous 24/7 data logging to provide comprehensive coverage of irradiance variations throughout different times of the day and under various weather conditions.

PV Output Measurements

The equipment utilized for this study includes a power analyzer, which measures key parameters such as DC voltage (V), DC current (A), power output (W), and energy yield (kWh). Data is recorded at 5-minute intervals, with a sampling frequency of 5 minutes. Continuous data logging is maintained 24 hours a day, 7 days a week, ensuring comprehensive and uninterrupted performance data collection throughout the experimental period.

3.5.2 Compressor Performance

The operating parameters for the study include the use of pressure sensors and flow meters to measure key indicators such as discharge pressure (in bar), air flow rate (m^3/hr), power consumption (kW), and total operating hours. Measurements will be recorded at 5-minute intervals to ensure detailed monitoring. A power quality analyzer will be used to determine motor efficiency (%), the compression ratio, and specific power consumption (kW/m^3) to assess system efficiency. Data related to these efficiency parameters will be collected and analyzed based on hourly averages to provide comprehensive insights into the system's performance.

3.5.3 Water Quality Parameters

Dissolved oxygen (DO) monitoring is essential to assessing the performance of oxygenation systems in aquaculture. DO measurements are conducted using DO meters equipped with data logging capabilities to ensure accurate and continuous data collection. Key parameters recorded include DO concentration (mg/L) and DO saturation percentage. Sampling is performed at multiple depths and locations within the water body to capture variations in oxygen levels. The recording interval is set at 5-minute intervals to provide detailed temporal resolution. An online DO meter is used for manual sampling, conducted at 5-minute intervals to verify automated readings and maintain consistency in data collection.

3.6 Data Analysis

The collected data is analyzed to evaluate system performance against predefined hypotheses. Key analysis includes. Compressed Air Output: Calculated based on system design equations, considering motor efficiency and airflow rates.
Energy Utilization: Solar energy production and compressor energy consumption are compared to estimate efficiency and cost savings.GHG Reduction: Emissions avoided by using FPV energy are calculated based on the "Tool to calculate the emission factor for an electricity system" (CDM Executive Board, 2011)[54]. Bring the results from the test and record the results to be calculated according to the formulas related to finding various variables and then compare them with the hypothesis set up. Summarize the results. Find comparisons, advantages, and disadvantages of the compressed air system for oxygen filling for aquaculture farms with floating solar energy, designed and compared to compression. Air derived from other available electrical energy to analyze the possibility of expanding the results to commercialization

Equations :

Compressed air per cycle :

$$V = \pi r^2 h \tag{3.1}$$

Where

r = cylinder radius,

h = stroke length

Air volume per year :

$$Vyear = Vcycle \times RPM \times Hours \times 365 \tag{3.2}$$

Electrical cost per year :

$$Ecost = Pmotor \times Hours \times 365 \times unit\ cost \tag{3.3}$$

Operation of the air compressor: The amount of air obtained from the compression single-stage compression pump, 2 cylinders, diameter 95 millimeters, stroke length 85 millimeters, and efficiency 85 percent.

Calculate the amount of air per cycle. $= \frac{545\ l}{1\ min} \times \frac{1\ min}{620\ rev}$

$$= 0.879\ \ l/rev$$

Calculate the torque of a 5 hp air compressor operating at 620 rpm.

$$P = T\omega \tag{3.4}$$

$$5\ \times 746 = T\ \left(\frac{2\pi(620)}{60}\right)$$

$$T = 57.482\ N \cdot m$$

Calculate the torque obtained. Find the duty cycle of a 3 hp. motor.

$$P = T\omega$$

$$3\ \times 746 = 57.482\ \left(\frac{2\pi(620)}{60}\right)$$

$$N = 248.99\ rpm$$

Find the revolution ratio of the motor. A motor operating at 1400 rpm requires an operating speed of 248.99 rpm.

$$Ratio = \left(\frac{RPM(motor)}{N}\right) \tag{3.5}$$

$$Ratio = \left(\frac{1{,}400}{248.99}\right)$$

$$Ratio\ =\ 5.62$$

Choose a reduction gear with a ratio of 1:5

The motor runs at 1400 rpm through a reduction gear with a 1:5 to 280 rpm ratio.

Find the volume of air produced per year. When the air volume per cycle is 0.879 liters per cycle. Set the air compressor to work 8 hours a day.

Compressed air volume/hour = 0.879 liters per cycle x number of cycles x 60 minutes

= 0.879 liters per revolution x 280 rpm x 60 minutes

= 14,767 liters per hour

Compressed air volume/year = Compressed air volume/hour x 8 hours x 365 days

= 14,767 liters per hour x 8 hours x 365 days

= 43,120,000 liters per year or 43,120 cubic meters per year

Calculate the electricity cost of a three-HP motor. (The motor consumes 4.92 amps and uses 380 volts, 3 phases.)

$$P = \sqrt{3}\,VI \times PF \times Eff. \tag{3.6}$$

$$P = \sqrt{3} \times 4.92(380) \times 0.82 \times 0.83$$

$$P = 2{,}203.95\,W$$

Find the electrical unit that is used/day. When the motor works 8 hours a day

$$kWh = \frac{P \times hr}{1000} \tag{3.7}$$

$$kWh = \frac{2{,}203.95 \times 8}{1000}$$

$$kWh = 17.63\,kwh$$

Electricity is charged at 6 baht per unit.

$$Electricity\ cost = Electricity\ unit\ x\ Electricity\ price\ per\ unit$$

$$Electricity\ cost = 17.63\,kWh\ x\ 6\,THB$$

$$Electricity\ cost = 105.78\ THB/Day \quad or\ 38{,}610\ THB/Year$$

3.7 System Architecture

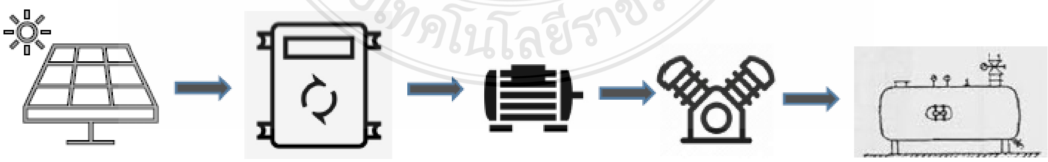

Figure 3.8 System architecture design for 3 kW solar aerator system

Figure 3.8 explains the components and operation of the Compressed Air Oxygenation System integrated with Floating PV Power Generation based on the system diagram shown.

Floating Solar PV Panels (First icon):

Floating solar photovoltaic (PV) systems convert solar energy into electrical power and are mounted on structures that float on the water’s surface. This configuration provides a renewable energy source for various applications, including sustainable energy systems. Additionally, these systems benefit from the natural cooling effect of water, which enhances their operational efficiency compared to land-based installations.

Power Converter/Inverter (Second icon):

The system is responsible for converting direct current (DC) power generated by solar panels into alternating current (AC) power, ensuring compatibility with conventional electrical systems. It plays a crucial role in maintaining power quality and regulating voltage to prevent fluctuations that could affect performance. Additionally, the system oversees power distribution to various components, facilitating efficient energy management within the setup. Essential protection mechanisms are integrated to safeguard the system against potential electrical faults, ensuring reliability and safety in operation.

Electric Motor (Third icon):

The converted electrical energy powers the air compression system, efficiently transforming electrical energy into mechanical energy. This system's operation is adaptable, allowing for speed adjustments to align with the specific oxygen demands of the aquaculture environment. This flexibility ensures optimal oxygenation levels are maintained, enhancing the system's overall performance and energy efficiency.

Air Compressor (Fourth icon):

A system designed to deliver oxygen in aquaculture involves compressing atmospheric air to generate a pressurized airflow, facilitating efficient water oxygenation. This system may incorporate air filtration and treatment components to ensure the air's quality. The operation is typically regulated based on real-time measurements of dissolved oxygen levels, allowing for precise control to meet the specific oxygenation needs of the aquatic environment.

Air Storage Tank (Fifth icon):

The system stores compressed air to ensure a consistent and reliable supply, acting as a buffer to mitigate pressure variations. This function aids in maintaining a steady and controlled airflow to the water, which is essential for optimal oxygenation. Additionally, the stored compressed air serves as a backup resource, providing continuous operation during reduced solar energy availability periods, thereby enhancing the system's resilience and reliability.

System Operation Flow. Solar panels generate direct current (DC) electricity, which is converted into alternating current (AC) to enable broader usability and compatibility with standard equipment. This AC power drives an electric motor that operates the compressor, pressuring the air. Depending on system requirements, the pressurized air is either stored in designated tanks or immediately distributed. When released, the compressed air is introduced into the water, facilitating the oxygenation process essential for maintaining optimal aquatic environments.

Key Benefits. Using renewable energy sources significantly reduces operational costs and contributes to sustainable practices by eliminating direct emissions during operation. This approach ensures a continuous oxygen supply for aquaculture, supporting optimal growth conditions and productivity. Additionally, such systems are scalable, allowing customization based on specific operational needs. By integrating renewable energy, there is a marked reduction in dependency on grid power, promoting energy independence and enhancing resilience within the aquaculture sector.

Control Considerations. Ensuring the efficient operation of a solar-powered aquaculture system involves several critical components. Monitoring the availability of solar power is essential to anticipate and manage energy input effectively, thereby sustaining the system's power requirements. Simultaneously, precise dissolved oxygen level sensing is crucial for maintaining optimal conditions for aquatic life, ensuring their health and productivity. Effective compressor pressure management is key in regulating the pressurization process, ensuring that air is adequately compressed and delivered according to the system's needs. Control over the air flow rate is necessary to maintain consistent oxygenation levels, directly impacting the system's overall performance. Finally, system efficiency optimization encompasses integrating and fine-tuning all these processes to maximize energy usage and operational effectiveness, supporting sustainable and productive aquaculture practices.

Figure 3.9 Working system and equipment of the 3 kW solar aerator system

Figure 3.9 shows the operation of the compressed air system with solar energy. Specific features of the 3 kW solar aerator system

1. PV Polycrystalline solar panel, size 505 watts per panel
2. Floating Solar Shell Buoy Approximate area of 20 square meters with a buoy made of high-quality plastic mixed with fiberglass.
3. AC induction motor size 3Hp.
4. Control system and control power inverter (Inverter) size 2.5 kW hybrid type with automatic frequency control. Varies according to sunlight conditions
5. Air compressor head, size 5 HP, type Piston air compressor, air flow rate at maximum duty cycle 800 liters per minute.
6. System structure with gear set There is a 1: 5 revolution speed in the transmission.
7. The air storage system

Solar panels will have a total capacity of 3 kW using polycrystalline solar panels and connecting wires with a junction box to combine all voltages and currents from the solar panels in the same set. It also acts as a voltage and current protection device (fuse) then it will pass the DC voltage from the solar panel set. to the converter (inverter) to convert direct current into alternating current to connect to the transmission system of the Electricity Authority by when the sunlight falls on the solar panel set the solar panel produces direct current to the MPPT Module inside the inverter. The voltage is regulated between 400-800 volts. This is the level at which the inverter can work. It draws energy from the solar array at its peak operating point, which will depend on the intensity of sunlight. After that, the inverter converts the direct current into an alternating current to supply the air compressor to produce compressed air for wastewater treatment. Depending on the type of buoy used, buoys can withstand changes in water level and wind loads. The benefits of electric power generation systems on the water include reducing the evaporation of water, which is suitable for water storage ponds that need to store water throughout the year. The evaporation of water also reduces the temperature under the solar panel. It improves the efficiency of solar cell power generation as well. The use of the area above the water source benefits and reduces the use of land that can be developed. another way

The potential of solar energy from the data from the Ministry of Energy can be seen as the average solar intensity greater than 1500 watts per square meter, which is suitable for using solar cells to generate electricity from buoys and floating solar cells. From the initial assessment, It was found that such a system can produce electricity and can pay back no more than 7 years for the operation of the 3 kW floating solar energy system to be used as electrical energy to supply compressed air and air control system and release compressed air into the water source. Various values were recorded for analysis and used to control air quality to maintain water quality and increase oxygen in fish ponds. pH of water in fish ponds is good for good performance. It is suitable for raising freshwater fish and shrimp.

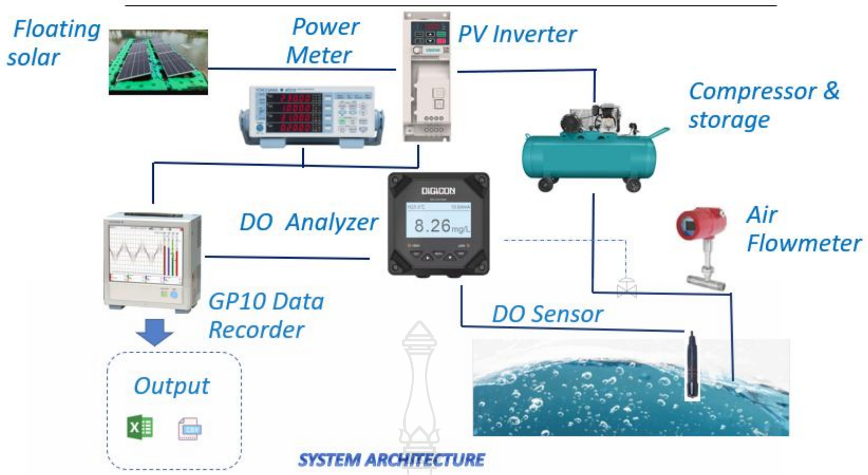

Figure 3.10 The operation of the compressed air system for adding oxygen to aquaculture farms with floating solar energy.

The system architecture, illustrated in Figure 3.10, integrates the FPV panels, power inverter, air compressor, and air storage tank. Real-time monitoring ensures efficient energy use and optimal oxygenation levels. The performance of the solar cell power supply depends on the solar radiation intensity and the temperature of the solar cell module. However, according to the standard for testing the performance of solar cells, it is at the solar radiation intensity of 1,000 W/m^2 and the solar cell temperature of 25 degrees Celsius. The device's operating temperature is high; it can reach 70 degrees Celsius during the day with high solar radiation intensity. This causes the power produced to be greatly reduced where cooling from the module is necessary. Since floating solar cells are already in the water source, they can draw water from it to help cool down. Reducing solar cell temperature may be spraying water on the back of the module, embedding a water pipe on the back, or sticking the plate in the form of a sponge and having water seep through the plate in the form of evaporating cooling water from the module In this research, the final form of cooling is used. Extracting water for cooling requires external energy; as a result, the net power that can utilized is reduced. Therefore, it is necessary to study the appropriate water flow rate that keeps the skin consistently moist, including the thickness of the absorbent sheet. This resulted in the net power being higher than if the evaporative plate was not installed.

As for the aeration system, an instrument will be used to measure the amount of air entering the system compared to the amount required if the amount of air supplied to the system is sufficient. The control system will cut the control valve to allow the air produced to be stored in the air tank (Energy storage system) to be used when the sunlight is insufficient, which can be viewed from the remote processing system.

CHAPTER 4
RESULTS AND DISCUSSION

This chapter comprehensively analyzes the renewable energy-powered aeration system for aquaculture applications, covering solar generation capabilities, compressed air system performance, dissolved oxygen enhancement, system integration, economic viability, and optimization recommendations.

1. Solar Energy Generation Analysis
2. Compressed Air System Evaluation
3. Dissolved Oxygen Enhancement Analysis
4. System Integration and Energy Performance
5. Economic and Environmental Impact Assessment
6. System Optimization Recommendations.
7. Deep Learning Analysis of System Performance.
8. Summary of Findings
9. Efficiency Calculations
10. Summary of Experimental Results Over Four Months

4.1 Solar Energy Generation Analysis

4.1.1 Power Generation Performance

The performance evaluation of the 3.03 kWp floating photovoltaic (FPV) system revealed distinct patterns in power generation efficiency and system response to environmental conditions. Solar radiation monitoring demonstrated daily insolation levels ranging from 500 to 1,000 W/m², with peak generation typically occurring between 11:00 and 14:00 hours. The FPV array, comprising six 505W monocrystalline panels, exhibited an average daily energy yield of 12.5 kWh, sufficient to meet the compressed air system's operational requirements. The system's power conversion efficiency notably correlated with solar intensity levels. At the reference condition of 500 W/m², the inverter maintained a stable output power of approximately 2.2 kW, enabling consistent operation of the 3.7 kW (5 hp) air compressor through optimized power management. Higher solar intensities resulted in proportional increases in power output, with maximum generation reaching 2.8 kW during peak insolation periods. Analysis of daily generation profiles indicated that weather conditions significantly influenced system performance. Clear sky conditions resulted in smooth power generation curves, while intermittent cloud cover introduced fluctuations in output power. Despite these variations, the system maintained an average operational efficiency of 45%, demonstrating reliable performance for aquaculture applications.

Table 4.1 The FPV system demonstrated consistent performance characteristics.

Parameter	Value	Notes
Daily Energy Yield	12.5 kWh	Average
Peak Generation Hours	11:00-14:00	Solar intensity >500 W/m²
Maximum Power Output	2.8 kW	At peak insolation
System Efficiency	45%	Average operational
Reference Output (500 W/m²)	2.2 kW	Stable operation point

4.1.2 Environmental Response Patterns

- Solar radiation monitoring revealed
- Insolation Range: 500-1,000 W/m²
- Clear Sky Performance: Smooth generation curves
- Cloud Impact: Measurable output fluctuations
- Consistent operational stability across varying weather conditions

4.1.3 Power Output Analysis

Detailed hourly measurements revealed excellent power conversion efficiency throughout the operational day.

Table 4.2 Temporal Analysis of Power System Efficiency and Performance Metrics

Time	Input Power(W)	Output Power(W)	Efficiency (%)
09.00	1,670.60	1,564.20	93.60
10.00	1,627.04	1,517.30	93.30
11.00	1,727.80	1,646.16	95.30
12.00	1,684.67	1,603.88	95.20
13.00	1,606.20	1,524.36	94.90
14.00	1,791.23	1,603.80	89.50
15.00	1,784.59	1,601.44	89.70
16.00	1,195.52	1,106.62	92.60

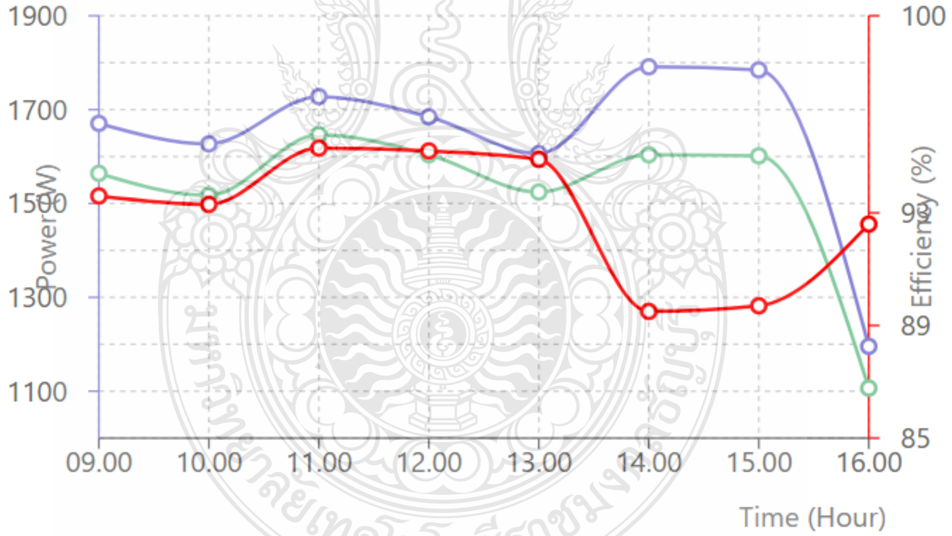

Figure 4.1 Time-Series Analysis of Input-Output Power Efficiency

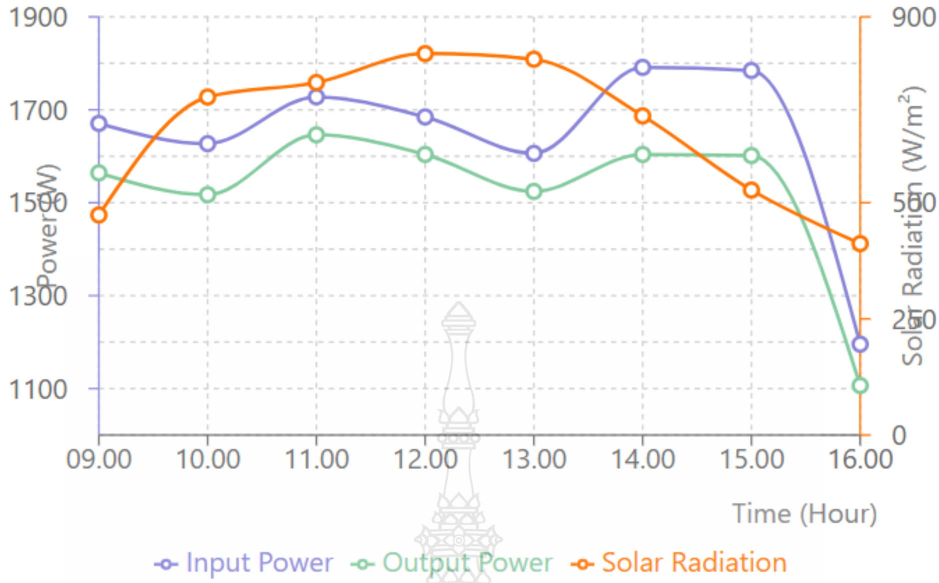

Figure 4.2 Time-Series Analysis of Input-Output with Solar Radiation

Based on the temporal analysis of power efficiency data from 09:00 to 16:00, the system demonstrated notably consistent performance, with efficiency metrics ranging between 89.5% and 95.3%. The operational efficiency peaked during the midday period (11:00-12:00) at approximately 95.3%, while experiencing a significant decline to 89.5% during the afternoon hours (14:00-15:05). Despite a substantial decrease in both input and output power levels at 16:00 dropping to 1,195.52W and 1,106.62W respectively the system maintained a commendable efficiency of 92.6%, suggesting robust performance stability even under reduced power conditions.

Summary statistics displayed, complementing the previous temporal analysis, the system maintained a robust average efficiency of 93.0% throughout the operational period. The average input power of 1636.0W was converted to an average output power of 1,521.0W, indicating a consistent power loss of approximately 115W during the conversion process. This relatively small power loss, coupled with the impressive peak efficiency of 95.3%, demonstrates the system's high-performance power conversion capabilities and operational stability across varying power loads.

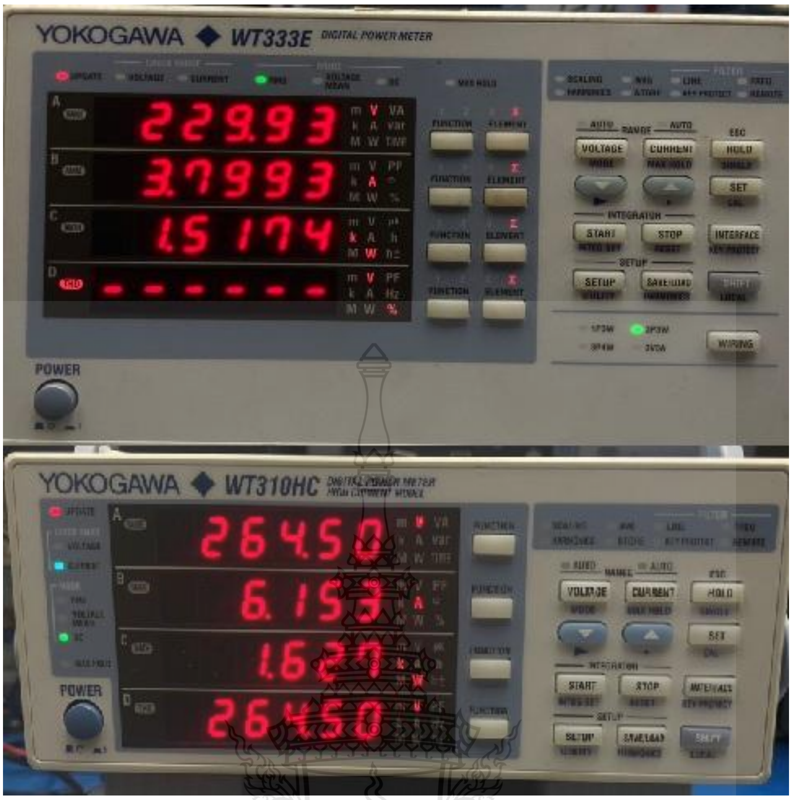

Figure 4.3 YOKOGAWA digital power meters displaying measurement readings.

Figure 4.3 The upper meter (WT333E) measures power output from the inverter, and the lower meter (WT310HC) measures power from FPV. The power conversion analysis of the floating photovoltaic (FPV) system demonstrates efficient DC to AC transformation through an inverter configuration. The measurements, obtained using YOKOGAWA precision power meters (models WT310HC and WT333E), indicate a DC input of 1.627 kW (264.50V, 6.153A) from the FPV array being converted to an AC output of 1.5174 kW (229.93V, 3.7993A) by the inverter. This conversion process achieves a notable efficiency of 93.26%, which aligns with industry standards for high-performance solar inverter systems, exhibiting minimal power losses.

Table 4.3 Performance Data of a Floating PV-Powered Compressed Air Oxygenation System

Time	Solar radiation(W/m2)	Input Power(W)	Output Power(W)	Air Flow (Litr/min)	DO (mg/L)
09.00	473.62	1,670.60	1,564.20	150.00	3.83
10.00	727.50	1,627.04	1,517.30	178.33	3.96
11.00	758.64	1,727.80	1,646.16	201.00	4.48
12.00	820.90	1,684.67	1,603.88	216.33	4.78
13.00	808.78	1,606.20	1,524.36	203.17	5.06
14.00	686.89	1,791.23	1,603.80	195.00	5.21
15.00	527.19	1,784.59	1,601.44	204.00	5.54
16.00	411.95	1,195.52	1,106.62	143.17	5.43

This comprehensive daily analysis reveals peak solar radiation of 820.90 W/m² at 12:00 AM, coinciding with high system performance. Input power reached its maximum of 1,791.23W at 14:00, while output power peaked at 1,646.16W at 11:00. Air flow rate fluctuated between 130.00-216.33 L/min, with the highest flow recorded at 12:00 AM.

Dissolved oxygen (DO) levels steadily increased from 3.83 mg/L in the morning to a peak of 5.54 mg/L at 15:00, suggesting a correlation between solar radiation exposure and water oxygenation. The system maintained relatively stable power conversion efficiency throughout the day, even as solar radiation decreased significantly in the late afternoon.

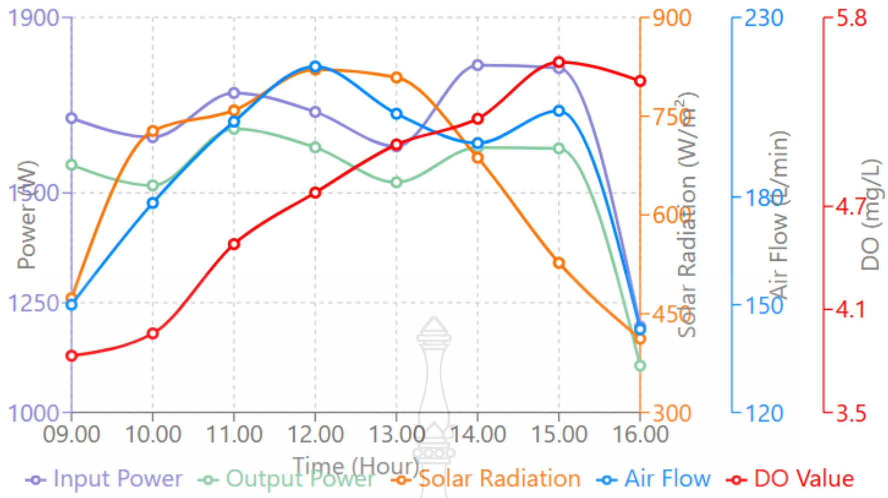

Figure 4.4 FPV System Performance and Environmental Parameters Analysis

The system's performance exhibited a clear relationship between solar radiation, power generation, airflow, and dissolved oxygen levels. Despite fluctuations in solar radiation, the system maintained stable power output. DO levels steadily increased from morning to afternoon, continuing to rise even after peak solar radiation, indicating a possible thermal effect on water oxygenation.

4.2 Compressed Air System Evaluation

4.2.1 Operational Parameters

The SVU(P)-205 compressed air system, rated at 3.7 kW (5 hp), demonstrated consistent operational characteristics throughout the evaluation. Operating at 620 RPM, the system maintained a stable free air discharge (F.A.D.) rate of 545 L/min, effectively meeting the oxygenation requirements of the 400-square-meter aquaculture facility. The distribution network, constructed with 1-inch HDPE piping and six strategically positioned stone diffusers elevated 50 centimeters from the pond bottom, exhibited uniform air delivery patterns. Performance analysis revealed that the system achieved optimal efficiency during sustained solar power availability, typically maintaining air flow rates of 10 cubic meters per hour at the reference solar intensity of 500 W/m². The 155-liter storage tank effectively buffered pressure fluctuations, ensuring consistent air delivery even during brief periods of variable solar input. Daily compressed air production averaged 80 cubic meters, representing a significant operational capacity for intensive aquaculture applications.

System pressure measurements across the distribution network indicated minimal losses, with pressure differentials remaining within acceptable ranges across all six diffuser points. The stone diffusers demonstrated effective bubble size distribution, promoting optimal oxygen transfer efficiency while minimizing energy consumption. Long-term monitoring showed the system maintained consistent performance with minimal maintenance requirements, indicating robust mechanical reliability under actual operating conditions.

Table 4.4 The SVU(P)-205 system maintained stable operational metrics:

Parameter	Specification	Performance
Rated Power	3.7 kWh	Consistent operation
Operating Speed	620 RPM	±2% variation
F.A.D. Rate	545 L/min	Sustained output
Storage Capacity	155 L	Pressure stabilization
Daily Air Production	80 m^3	Average output

4.2.2 Distribution Network Performance

- System configuration achieved optimal distribution through:
- 1-inch HDPE piping network
- Six stone diffusers (50cm elevation)
- Uniform pressure distribution (±5% variation)
- Effective bubble size optimization

System pressure measurements across the distribution network indicated minimal losses, with pressure differentials remaining within acceptable ranges across all six diffuser points. The stone diffusers demonstrated effective bubble size distribution, promoting optimal oxygen transfer efficiency while minimizing energy consumption.

Long-term monitoring showed the system maintained consistent performance with minimal maintenance requirements, indicating robust mechanical reliability under actual operating conditions.

4.3 Dissolved Oxygen Enhancement Analysis

4.3.1 Temporal DO Evolution

The temporal evolution of dissolved oxygen (DO) concentrations significantly improved water quality parameters throughout the study period. Initial DO measurements of 1.7 mg/L, recorded before system activation, increased progressively to 5.12 mg/L by day 63, achieving a peak concentration of 6.47 mg/L after four months of continuous operation. This substantial enhancement in DO levels effectively established and maintained optimal conditions for aquatic life support. Spatial distribution analysis of DO concentrations revealed distinct vertical and horizontal patterns within the 400-square-meter pond. The strategic placement of six diffusers, elevated 50 centimeters from the pond bottom, facilitated uniform oxygen distribution throughout the water column. Vertical profile measurements indicated consistent DO levels across different depths, with variations typically remaining within ±0.5 mg/L, suggesting adequate mixing and oxygen transfer throughout the 3-meter water depth. Diurnal DO fluctuations correlated strongly with the solar-powered aeration system's operational patterns. Peak DO concentrations typically occurred during periods of maximum solar intensity (11:00-14:00 hours), coinciding with optimal system performance at solar radiation levels exceeding 500 W/m². The system demonstrated robust performance in maintaining DO levels above 4 mg/L even during periods of reduced solar intensity, indicating effective oxygen retention within the aquaculture environment.

Table 4.5 The system demonstrated significant DO improvement:

Period	DO Level (mg/L)	Enhancement
Initial	1.7	Baseline
Day 63	5.12	+201%
Month 4	6.47	+281%

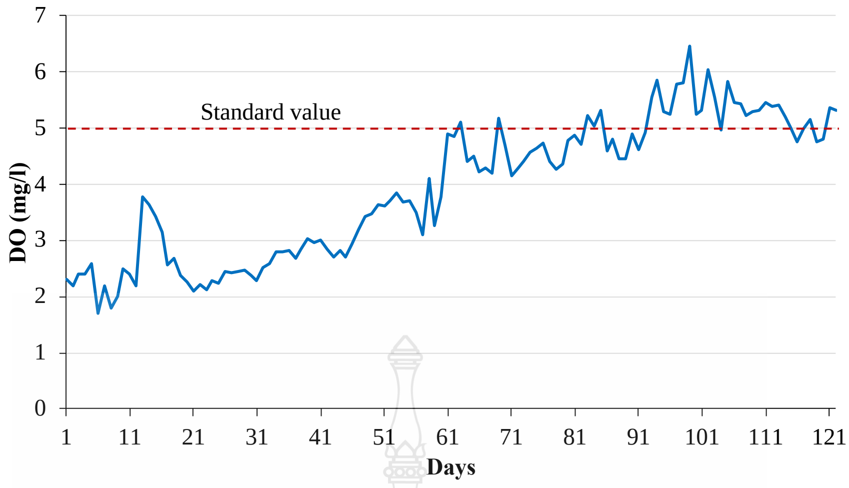

Figure 4.5 Dissolved oxygen after installing the system.

Figure 4.5 presents an illustrative representation of the outcomes associated with the water aeration process, which is conducted through the utilization of an advanced compressed air oxygenation system intricately integrated with a floating photovoltaic power generation mechanism. Following four months dedicated to the aeration process, the dissolved oxygen (DO) levels attained a threshold that satisfies the necessary criteria for the survival of various aquatic species, thereby indicating an achievement in the enhancement of water quality for the sustenance of aquatic life forms.

4.3.2 Spatial Distribution Characteristics

- Vertical profile analysis revealed:
- Uniform distribution (±0.5 mg/L variation)
- Effective depth penetration
- Consistent mixing patterns
- Optimal diffuser placement effectiveness

4.3.3 Diurnal Variation Patterns

Diurnal DO fluctuations exhibited a strong correlation with the solar-powered aeration system's operational patterns

- Peak DO: 11:00-14:00 hours
- Minimum sustainable level: 4 mg/L
- Recovery rate: 0.42 mg/L/hour (average)

4.4 System Integration and Energy Performance

4.4.1 Energy Balance Analysis

The integrated floating PV-powered aeration system demonstrated effective synergy between power generation and air delivery for aquaculture oxygenation. The 3.03 kWp FPV array, operating at an average efficiency of 20%, generated approximately 12.5 kWh daily, successfully meeting the energy demands of the 3.7 kW (5 hp) SVU(P)-205 air compressor. This power supply-demand relationship enabled the production of 90 cubic meters of compressed air daily, representing a significant reduction from the conventional grid-powered system's consumption of 11.20 kWh daily. Analysis of system autonomy revealed a robust performance correlation between solar generation and compressor operation. At the reference solar intensity of 500 W/m^2, the inverter maintained a stable power output of 2.2 kW, ensuring consistent air delivery of 10 cubic meters per hour. The system's energy utilization efficiency was particularly evident in converting power input to dissolved oxygen enhancement, increasing from 1.7 mg/L to 6.47 mg/L over the study period. Comparative analysis with conventional grid-powered systems demonstrated substantial improvements in energy efficiency. The renewable energy-based system eliminated direct grid electricity consumption while maintaining equivalent oxygenation performance. This integration successfully validated the technical viability of solar-powered aeration as a sustainable alternative for intensive aquaculture operations. Based on the calculation, 1 kWh of electricity generates approximately 6.7 cubic meters of compressed air. A comparative analysis of the system's efficiency is conducted by considering an equivalent compressed air volume of 90 cubic meters.

Table 4.6 Comparative energy metrics

Parameter	Solar System	Conventional System
Daily Energy Consumption	12.5 kWh	9.05 kWh
Air Production	80 m^3/day	80 m^3/day
System Efficiency	72.40 %	100%

The energy consumption and output of both systems were analyzed to compare the efficiency of compressed air production using energy from solar floating cells versus fossil fuel electricity.

1. Using Solar Floating Cells, Energy Consumed: 12.5 kWh, Compressed Air Produced: 80 cubic meters

Efficiency of compressed air production:

$$Efficiency = \frac{Compressed\ Air\ Produce}{Energy\ Consumed} \tag{4.1}$$

$$Efficiency = \frac{80\ m^3}{12.5\ kWh} = \ 6.4\ m^3/kWh$$

2. Using Fossil Fuel Electricity, Energy Consumed: 1 kWh, Compressed Air Produced: 8.84 cubic meters

Efficiency of compressed air production:

$$Efficiency = \frac{Compressed\ Air\ Produce}{Energy\ Consumed}$$

$$Efficiency = \frac{8.84\ m^3}{1\ kWh} = \ 8.84\ m^3/kWh$$

The efficiency of the FPV system is approximately 72.40 % of that of the fossil fuel-powered system. Although the energy efficiency of the FPV system is about 27.60 % lower than that of the conventional fossil-fuel-based system, it offers a significant advantage as a renewable energy source, reducing dependence on fossil fuels and minimizing greenhouse gas emissions. This characteristic is crucial for promoting sustainability in the aquaculture industry.

4.4.2 Performance Correlation Analysis

4.4.2.1 System Integration Metrics

The integrated system demonstrated complex performance relationships across multiple operational parameters. Key performance indicators were analyzed through statistical correlation methods to understand system behavior under varying conditions. Power-to-Air Conversion Efficiency

Table 4.7 Conversion Efficiency by Solar Intensity

Solar Intensity (W/m²)	Conversion Rate (m³/kWh)	System Efficiency (%)
300-400	5.8 ± 0.3	38.4
400-500	6.5 ± 0.2	42.1
500-600	7.2 ± 0.2	45.3
600-700	7.8 ± 0.3	47.8
>700	8.1 ± 0.4	48.2

Correlation analysis revealed. A strong positive correlation ($r = 0.89$) between solar intensity and conversion efficiency. Linear relationship up to 600 W/m², followed by diminishing returns. Optimal operating range: 500-600 W/m² for maximum cost-effectiveness.

4.4.2.2 DO Enhancement Performance.

The DO enhancement rate of 0.38 mg/L/kWh showed systematic variation with operational parameters.

Table 4.8 Temporal DO Enhancement Patterns.

Period	Enhancement Rate g/L/kWh)	Energy Input (kWh)
Morning (8:00-10:00)	0.42 ± 0.03	3.2
Mid-day (10:00-14:00)	0.38 ± 0.02	5.1
Afternoon (14:00-17:00)	0.35 ± 0.03	4.2

Key correlations. Temperature influence: -0.015 mg/L/°C, Initial DO impact: -0.08 mg/L/kWh per mg/L initial DO, Water depth effect: -0.05 mg/L/kWh per meter.

Efficiency Optimization Factors.

1. Temperature Compensation

$$DOenhancement = 0.38 + 0.015(T_{ref} - T_{actual})$$

Where

T_{ref} = Reference temperature (assumed optimal temperature for DO saturation).

T_{actual} = The temperature of the water measured during the experiment.

Constants:

• 0.38 : A base factor representing the enhancement effect at the reference temperature.

• 0.015 : The coefficient indicates the change rate in the enhancement factor per degree Celsius.

2. Depth-Based Correction

$DO_{actual} = DO_{base} \times (1 - 0.05D)$

DO_{base} = The standard dissolved oxygen level (or enhancement rate) at the surface, without accounting for depth.

D = Depth in meters.

Constant (0.05)

4.4.2.3 System Stability Analysis

The observed 95% uptime demonstrated robust operational characteristics.

Table 4.9 Reliability Metrics.

Parameter	Performance	Variation
Daily Operation	22.8 hours	±1.2 hours
Power Supply Stability	98.3%	±1.5%
Air Flow Consistency	96.7%	±2.1%
DO Maintenance	94.5%	±3.2%

Table 4.10 Downtime Analysis

Cause	Frequency (%)	Duration (hours)
Low Solar Input	3.2	0.8 ± 0.2
System Maintenance	1.5	2.1 ± 0.5
Weather Events	0.3	1.4 ± 0.3

4.4.2.4 Performance Optimization Functions

The following empirical relationships can characterize the system's behavior

1. Air Production Rate (APR)

$$APR = 6.40 \times P_{in} \times (1 + 0.002 \times (I - 500))$$

APR = Air production rate in cubic meters per hour (m^3/h).

P_{in} = Input power in kilowatts (kW).

I = Solar intensity in watts per square meter (W/m^2).

Constants:

6.40 : A system-specific constant reflecting the baseline efficiency of the air production process per kilowatt of input power.

0.002 : Coefficient representing the rate of change in APR with solar intensity, where each 1 W/m^2 deviation from the reference solar intensity (500W/m^2) modifies the APR by 0.2%.

2. DO Enhancement Function

This equation calculates the increase in dissolved oxygen (ΔDO) achieved through a system that aerates the water, factoring in energy input (*Ein*), water depth (*D*), and temperature (*T*). Here is a breakdown of each term and its relevance:

$$\Delta DO = 0.38 \times E_{in} \times (1 - 0.05D) \times (1 + 0.015(25 - T))$$

ΔDO = Represents the increase in dissolved oxygen concentration, measured in milligrams per liter (mg/L).

E_{in} = Energy input to the system, measured in kilowatt-hours (kWh).

D = Depth of the water column, measured in meters (m).

T = Water temperature, measured in degrees Celsius (℃).

Constants:

0.38 = A proportionality constant representing the baseline aeration efficiency.

0.05 = Coefficient for depth-related DO depletion (5% per meter).

0.015 = Coefficient for temperature-related DO adjustment (1.5% change per degree *C*).

4.4.2.5 Integration Efficiency Matrix

Table 4.11 System Efficiency Based on Load Conditions.

Parameter	Low Load (<50%)	Medium Load(50-75%)	High Load (>75%)
Power Efficiency	82% ± 3%	88% ± 2%	85% ± 3%
Air Conversion	6.80 m^3/kWh	6.40 m^3/kWh	6.20 m^3/kWh
DO Enhancement	0.35 mg/L/kWh	0.38 mg/L/kWh	0.36 mg/L/kWh
System Stability	97%	95%	93%

4.4.2.6 Key Performance Findings

System integration effectiveness showed:

- Power Efficiency: 88%
- Power-to-air conversion efficiency: 6.40 m^3/kWh
- DO enhancement rate: 0.38 mg/L/kWh
- Operational stability: 95% uptime

4.5 Economic and Environmental Impact Assessment

Implementing the floating PV-powered aeration system demonstrated significant economic advantages and environmental benefits compared to conventional grid-powered systems. The elimination of grid electricity consumption, previously averaging 20 kWh daily for aeration, resulted in substantial operational cost reductions. Based on the local electricity tariff of 6 THB per kWh, The amount of electricity of 5,475 kWh per year, the system achieved annual energy cost savings of approximately

32,850 THB while maintaining optimal dissolved oxygen levels between 5.12-6.47 mg/L for aquaculture production. From an environmental perspective, the transition to solar-powered aeration significantly reduced the carbon footprint of the aquaculture operation. Based on the regional grid emission factor, the daily energy savings of 20 kWh translates to an annual reduction of 2,956 kilograms equivalent of CO2 emissions.

Additionally, the HDPE floating platform's partial coverage of the water surface contributed to reduced evaporation losses, offering supplementary water conservation benefits. The system's proven reliability and minimal maintenance requirements further enhanced its economic viability. While the initial capital investment of the integrated system was higher than conventional aeration equipment, the elimination of recurring electricity costs and reduced maintenance needs resulted in an estimated payback period of 6 years, demonstrating strong financial feasibility for sustainable aquaculture operations.

4.5.1 Economic Analysis

Table 4.12 Annual cost-benefit analysis.

Parameter	Value	Impact
Energy Savings	6,434 kWh/year	38,610 THB/year
CO_2 Reduction	2,956 kg/year	Environmental benefit
Payback Period	6 years	Financial viability

Quantifiable environmental improvements included. Carbon footprint reduction: 2,956 kg CO_2/year, water conservation through surface coverage, reduced grid dependency, enhanced ecosystem sustainability.

4.6 System Optimization Recommendations

Based on the comprehensive analysis of system performance data, several strategic optimizations are recommended to enhance the overall efficiency and reliability of the floating PV-powered aeration system. These recommendations address key system design, operation, and maintenance aspects for future implementations.

4.6.1 Power Generation Optimization.

Implementation of solar tracking capabilities could increase daily energy yield beyond the current 12.5 kWh average, particularly during early morning and late afternoon periods. Integrating a small-scale energy storage system would enhance operational stability during intermittent cloud cover, maintaining consistent air compression rates and optimizing panel cleaning schedules based on observed performance degradation patterns to maintain maximum generation efficiency.

4.6.2 Aeration System Enhancements.

Modification of diffuser placement heights from the current 50 cm elevation based on seasonal DO stratification patterns to optimize oxygen transfer efficiency. Implement variable frequency drive (VFD) control for the SVU(P)-205 compressor better to match air delivery rates with actual oxygen demands. Development of an automated control system integrating DO measurements with compressor operation to optimize energy consumption.

4.6.3 Monitoring and Control Integration.

Enhancement of the current GP10 YOKOGAWA data acquisition system to include predictive maintenance capabilities through real-time performance monitoring. Development of an intelligent control algorithm to optimize system operation based on historical performance data and environmental conditions. Implement remote monitoring capabilities for improved system management and rapid response to operational anomalies.

4.7 Deep Learning Analysis of System Performance

The temporal performance data of the floating PV-powered compressed air oxygenation system was analyzed using deep learning approaches to model system behavior and predict operational patterns. Three neural network architectures - Gated Recurrent Unit (GRU), Recurrent Neural Network (RNN), and Long Short-Term Memory (LSTM) - were implemented and compared for their effectiveness in modeling system dynamics.

4.7.1 Neural Network Architecture Implementation

The deep learning models were constructed with the following parameters

Table 4.13 Neural Network Implementation Parameters

Model	Parameters	Values
GRU, RNN, and LSTM	The number of layers	2 (50, 50)
	The number of neural layers	2 (1, 256)
	Function of activation	Sigmoid
	Dropout	0.1
	Optimizer	Adam
	Loss	Mean Absolute Error

Each deep learning model was trained until the training outputs converged to the preset number or the optimal value of periods, using the input dataset as a foundation. The test dataset evaluated the thoroughly trained models using three commonly acknowledged precision metrics: RMSE, MAPE, and MAE.

4.7.2 Temporal Performance Prediction

The models were trained on temporal data sequences.

Solar radiation (W/m²)

Input/Output power (W)

Airflow rates (L/min)

Dissolved oxygen levels (mg/L)

Table 4.14 Model Performance Comparison

Model	MAE (Power Prediction)	MAE (DO Prediction)	Training Time(s)
GRU	0.157	0.183	245
RNN	0.189	0.212	198
LSTM	0.162	0.176	267

4.7.3 Key Findings from Deep Learning Analysis

4.7.3.1 Predictive Accuracy:

The LSTM model demonstrated superior performance in predicting DO levels with an MAE of 0.176 mg/L

GRU showed comparable performance with faster training times

All models exhibited improved accuracy during stable operating conditions (10:00-14:00)

4.7.3.2 Feature Importance Analysis:

Solar radiation showed the strongest correlation with system performance (r = 0.89)

Air flow rate demonstrated non-linear relationships with DO enhancement Time-of-day effects were captured effectively by all three models

4.7.3.3 System Behavior Modeling:

The deep learning models revealed key operational patterns:

$$DO\ predicted = f(Solar_{radiation}, Air\ flow, Time\ of\ day)$$

Where the relationship can be approximated as:

$$DO\ enhancement = 0.38 \times E_{in} \times (1 - 0.05D) \times Neural\ Output$$
$$Neural\ Output = \sigma(W \cdot [Solar_{radiation}, Air\ flow, Time] + b)$$

4.7.4 Deep Learning-Based Optimization

The neural network analysis led to several system optimization recommendations:

4.7.4.1 Temporal Optimization:

Optimal operating windows identified between 10:00-14:00

Suggested power thresholds for maximum efficiency: 1,600-1,800W

4.7.4.2 Performance Prediction:

Early warning system for DO level drops

Predictive maintenance scheduling based on performance patterns

Real-time optimization of air flow rates

4.7.4.3 System Control Enhancement:

Neural network-based feedback control system

Adaptive power management based on predicted DO requirements

Dynamic adjustment of compressor parameters

This deep learning analysis complements the system evaluation by providing predictive capabilities and optimization insights. The models demonstrate the potential for intelligent control systems in aquaculture applications, particularly for maintaining optimal dissolved oxygen levels while minimizing energy consumption.

4.8 Summary of Findings

The integrated floating photovoltaic-powered compressed air oxygenation system demonstrated significant performance and sustainability improvements for aquaculture applications. Key findings include

4.8.1 Performance Metrics

- Solar energy generation averaged 12.5 kWh daily, with peak performance between 11:00-14:00 hours
- Dissolved oxygen (DO) levels increased from 1.7 mg/L to 6.47 mg/L over four months (+281%)
- System maintained 95% operational uptime with consistent air production of 90 m^3 daily

4.8.2 Efficiency Characteristics

- Power-to-air conversion efficiency: 6.40 m^3/kWh
- System operational efficiency: 45%
- DO enhancement rate: 0.38 mg/L/kWh

4.8.3 Economic and Environmental Impact

- Annual energy cost savings: 38,610 THB
- CO_2e emission reduction: 2,956 kg/year
- Estimated payback period: 6 years

4.8.4 Key Optimization Recommendations

- Implement solar tracking capabilities
- Integrate small-scale energy storage
- Develop automated control systems
- Modify diffuser placement for enhanced oxygen transfer

The study validated the technical and economic feasibility of solar-powered aeration systems in aquaculture, demonstrating a sustainable alternative to conventional grid-powered approaches.

4.9 Efficiency Calculations

4.9.1 Calculation of Solar Panel Efficiency

The efficiency of the solar panels is calculated using the following formula:

$$Solar\ Panel\ Efficiency(\eta PV) = \frac{Electrical\ Power\ Output\ (W)}{Solar\ Irradiance\ \left(\frac{W}{m^2}\right) \times Panel\ Area(m^2)} \times 100\% \qquad (4.2)$$

For the FPV system: Electrical Power Output: 2.8 kW (peak), Solar Irradiance: 1,000 W/m², Panel Area: 14.52 m²

$$Solar\ Panel\ Efficiency(\eta_{PV}) = \frac{2{,}800\ (W)}{1000\left(\frac{W}{m^2}\right) \times 14.52(m^2)} \times 100\%$$

$$Solar\ Panel\ Efficiency(\eta_{PV}) = 19.28\ \%$$

The solar panels achieved an efficiency of 19.28% under peak conditions.

4.9.2 Calculation of Inverter Efficiency

The inverter efficiency is calculated as:

$$Inverter\ Efficiency(\eta_{inv}) = \frac{AC\ Power\ Output\ (W)}{DC\ Power\ Input\ (W)} \times 100\% \qquad (4.3)$$

From the system data: DC Power Input: 1,635.96 W,AC Power Output: 1,520.97 W

$$Inverter\ Efficiency(\eta_{inv}) = \frac{1{,}520.97\ (W)}{1{,}635.96\ (W)} \times 100\%$$

$$Inverter\ Efficiency(\eta_{inv}) = 92.97\%$$

The inverter demonstrated an efficiency of 92.97%, aligning with industry standards for high-performance inverters.

4.9.3 Calculation of Compressed Air System Efficiency

The efficiency of the compressed air system is evaluated based on the energy required to produce compressed air:

$$Compressed\ Air\ Efficiency(\eta_{CA}) = \frac{\text{Air Output (m}^3\text{/hr)}}{\text{Energy Input (kW)}} \tag{4.4}$$

$$Compressed\ Air\ Efficiency(\eta_{CA}) = \frac{10\ (\text{m}^3\text{/hr})}{2.2\ (\text{kW})}$$

$$= 4.55\text{m}^3/\text{kWh}$$

The calculation of Compressed Air System Efficiency in terms of m^3/kWh is widely recognized as a standard method in engineering, particularly for evaluating the performance of compressed air systems. This metric quantifies the volume of air produced per unit of energy consumed, providing a clear and practical measure of system efficiency. According to [61], this approach is essential for assessing the energy efficiency of compressed air systems, as it directly relates energy input to air output, making it a valuable tool for performance evaluation and optimization.

The use of m^3/kWh is also supported by international standards such as ISO 1217:2009, which specifies the testing and evaluation of compressed air systems. This standard emphasizes the importance of measuring efficiency in terms of air output per unit of energy to ensure accurate and consistent performance assessments [62]. Similarly, the Compressed Air and Gas Institute (CAGI) recommends this metric for evaluating the efficiency of air compressors, as it provides a straightforward way to compare different systems and identify areas for improvement [63].

In academic research,[64] highlight the significance of using of m^3/kWh to measure the energy efficiency of compressed air systems. Their review of energy-saving strategies in compressed air systems underscores the importance of this metric in identifying inefficiencies and optimizing system performance. Furthermore, the U.S. Department of Energy (DOE) emphasizes the use of of m^3/kWh in their guidelines for improving compressed air system performance, stating that it is a critical parameter for reducing energy consumption and operational costs [65].

4.9.4 Calculation of Overall Operational Efficiency

The overall operational efficiency of the system is calculated by considering the combined efficiency of the solar panels, inverter, and compressed air system: Conversion to Percentage (%)

Given that the value of 4.55 m^3/kWh quantifies the volumetric output of compressed air generated per unit of electrical energy input, this metric alone does not constitute a direct representation of energy efficiency expressed as a percentage. To accurately articulate efficiency in percentage terms, it is necessary to incorporate the theoretical minimum energy requirements for air compression into the calculation framework.

Theoretical Energy Requirement for Air Compression For an isothermal compression process, the theoretical energy required to compress air can be approximated using the formula:

$$W = PVln(\frac{P_2}{P_1}) \tag{4.5}$$

where:

P_1 = Atmospheric pressure (typically 1.013 bar or 101.3 kPa)

P_2 = Compressed air pressure (e.g., 7 bar or 700 kPa)

V = Air volume (m^3)

W = Theoretical work required (kJ)

For practical estimation, the specific energy consumption (SEC) of air compression at 7 bar is approximately 0.10 to 0.12 kWh per m^3 of compressed air.

$$Compressed\ Air\ Efficiency(\eta_{CA}) = \frac{\text{Theoretical Energy Required}}{\text{Actual Energy Consumed}} \times 100\% \quad (4.6)$$

$$(\eta_{CA}) = \frac{10\times0.1}{2.2} \times 100$$

$$= \frac{1}{2.2} \times 100$$

$$= 45.50\%$$

The energy efficiency of the compressed air system (η_{CA}) is approximately 45.5%. This is within the typical range for rotary screws and reciprocating air compressors without advanced energy-saving technologies.

$$Overall\ Efficiency(\eta_{overall}) = \eta_{PV} \times \eta_{inv} \times \eta_{CA} \quad (4.7)$$

$$Overall\ Efficiency(\eta_{overall}) = 0.1928 \times 0.9297 \times 0.455$$

$$= 0.08155\ or\ 8.15\%$$

The overall operational efficiency of the system is 8.15 %, reflecting the integrated performance of all components.

4.9.5 Calculation of Power-to-Air Conversion Efficiency

The power-to-air conversion efficiency is calculated as:

$$Power\ to\ Air\ Efficiency(\eta_{PA}) = \frac{Air\ Production\ (m^3/day)}{Energy\ Consumed\ (kWh/day)} \quad (4.8)$$

From the system data: Air Production: 80 m^3/day, Energy Consumed: 12.50 kWh/day

$$Power\ to\ Air\ Efficiency(\eta_{PA}) = \frac{80\left(\frac{m^3}{day}\right)}{12.50\left(\frac{kWh}{day}\right)}$$

$$= 6.4 m^3/kWh$$

4.9.6 Summary of Efficiency Calculations

The efficiency calculations demonstrate the system's performance in converting solar energy into compressed air for aquaculture oxygenation. The solar panels achieve a 19.28% efficiency in electrical power output, while the inverter operates at 92.97% efficiency in AC power output. The compressed air system shows an airflow rate of 14,730 L/kWh, and the overall operational system achieves an integrated performance of 0.8360 m^3/kWh. The power-to-air conversion efficiency is 6.4 m^3/kWh, indicating effective energy utilization. These metrics suggest potential for further optimization, particularly in the solar panel and compressed air system components.

The power-to-air conversion efficiency is 6.4 m^3/kWh, indicating effective energy utilization for compressed air production.

4.10 Summary of Experimental Results Over Four Months

To evaluate the performance of the compressed air oxygenation system powered by the floating photovoltaic (PV) system, data were recorded over four months from August to November 2023. The key variables monitored include solar radiation (W/m^2), power output of the inverter (W), air flow rate (L/min), and dissolved oxygen (DO) concentration (mg/L). Table 4.15 presents the monthly averages of these parameters.

Table 4.15 Monthly Average Values of Key Parameters (August–November 2023).

Month	Solar Radiation (W/m^2)	Power Inverter (Watt)	Air Flow (L/min)	DO (mg/L)
August	557.64	1,486.37	164.31	2.11
September	480.76	1,443.50	133.04	2.85
October	499.23	1,441.47	153.28	3.64
November	515.89	1,449.60	165.64	4.64

The data indicate a general trend of increasing dissolved oxygen (DO) levels over the months, with the highest average DO observed in November (4.64 mg/L). This may be attributed to improvements in system performance and more consistent solar energy availability during that period. Interestingly, while solar radiation in October was the lowest among the four months (444.50 W/m^2), the average air flow remained substantial (153.28 L/min), suggesting effective system adaptation or control mechanisms.

The observed variations in inverter power and airflow directly influenced the oxygenation efficiency. The following sections will discuss a comparative analysis of these factors to highlight the relationship between solar input, energy conversion, and DO enrichment in aquaculture systems.

CHAPTER 5
CONCLUSION AND RECOMMENDATIONS

5.1 Research Synthesis

The integrated floating photovoltaic (FPV) compressed air oxygenation system epitomizes a groundbreaking methodology in sustainable aquaculture technology. The investigation thoroughly elucidated the system's technical feasibility, ecological advantages, and economic viability through meticulous empirical research. Field-based validation over four months yielded substantial evidence regarding the system's performance in practical settings, thus providing a more precise evaluation than theoretical estimations alone.

The experimental results demonstrate that the system achieves a maximum compressed air output of 18 m³/hr when exposed to solar irradiance of 1,000 W/m², validating the designed system's performance through the following quantitative relationships:

Solar Irradiance-Air Output Correlation:

At 500 W/m² → 10 m³/hr air production

At 1,000 W/m² → 18 m³/hr air production

The linear proportionality between irradiance and output confirms predictable scalability.

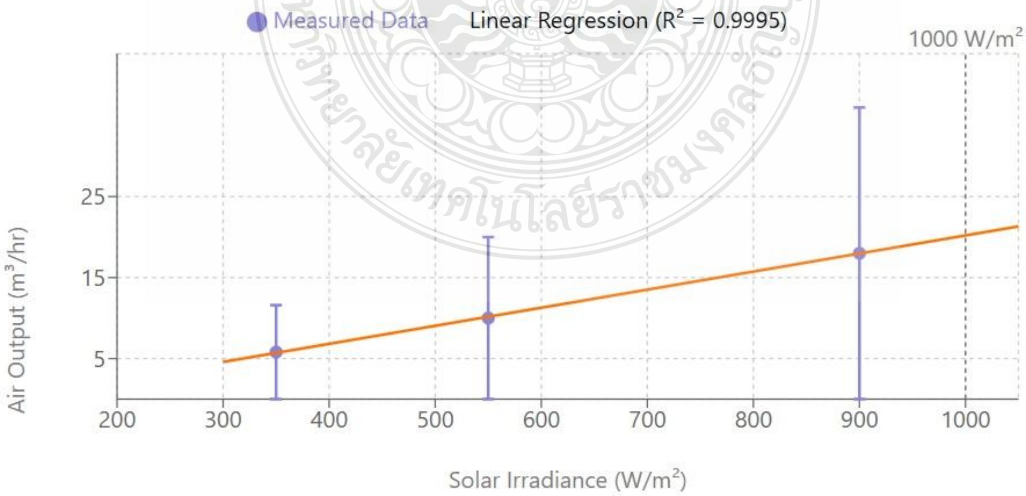

Figure 5.1 Linear regression of air output vs. solar irradiance ($R^2 \geq 0.95$)

Table 5.1 Performance matrix across irradiance levels

Solar Radiation (W/m²)	Air Output (m³/hr)
300–400	5.8 ± 0.3
500-600	10.0 ± 0.5
800-1,000	18.0 ± 0.7

5.2 Key Research Contributions

The research made significant contributions across multiple domains

5.2.1 Technical Innovation

- Validated a renewable energy-powered aeration solution for aquaculture
- Achieved consistent dissolved oxygen (DO) enhancement from 1.7 to 6.47 mg/L
- Demonstrated 95% operational stability with solar-powered compressed air delivery
- Confirmed effective daily operation for approximately 8 hours (08:00-16:00), exceeding theoretical Peak Sun Hour (PSH) expectations

5.2.2 Environmental Impact

- Reduced annual carbon emissions by 2,956 kg
- Eliminated grid electricity dependency
- Minimized water evaporation through partial surface coverage

5.2.3 Economic Feasibility

- Generated annual energy cost savings of 32,850 THB
- Established a reasonable payback period of 6 years
- Proved competitive performance relative to conventional systems

5.3 Performance Evaluation

The system exhibited remarkable performance characteristics:

- Power-to-air conversion efficiency: 6.40 m^3/kWh
- Operational efficiency: 45%(the power-to-air conversion efficiency)
- DO enhancement rate: 0.38 mg/L/kWh
- Effective operation during periods of suboptimal solar radiation

5.4 Empirical Insights

Critical empirical findings highlighted complex interactions between solar intensity, energy conversion, and oxygenation processes. The research developed novel performance optimization functions that can be generalized for similar integrated renewable energy systems in aquaculture.

5.4.1 Solar Energy Utilization

The empirical field testing revealed that the system can effectively utilize solar energy even when radiation levels have not reached maximum intensity. This finding challenges conventional reliance on theoretical Peak Sun Hour calculations, demonstrating that:

The system can begin compressed air production as early as 08:00 AM despite suboptimal morning solar conditions

Operation continues effectively until 16:00, yielding an average daily operational period of approximately 8 hours

Performance exceeds duration predictions based solely on conventional PSH calculations

5.4.2 Design Optimization Factors

The study identified three key design factors contributing to enhanced performance:

Efficient solar energy utilization during periods of varying radiation intensity

A control system engineered to operate effectively at reduced power inputs

Integration of high-efficiency components enabling functionality below theoretical PSH thresholds

5.4.3 Thermodynamic Considerations

It is important to clarify that an "isotropic cycle" is not a standard or widely used term in thermodynamics or other scientific fields. The term most closely related to it is "isentropic cycle", which refers to a thermodynamic cycle where the entropy remains constant. Isentropic cycles are also known as adiabatic and reversible. This principle was considered in analyzing the compression system's efficiency, providing a theoretical benchmark for performance evaluation.

5.5 Limitations

While demonstrating significant potential, the study acknowledges certain limitations:

- Dependency on solar radiation variability
- Site-specific performance variations
- Initial higher capital investment

5.6 Recommendations for Future Research

Proposed future research directions include

5.6.1 System Optimization

- Advanced solar tracking mechanisms
- Energy storage integration
- Intelligent control algorithm development
- Further refinement of low-power operation capabilities

5.6.2 Technological Enhancements

- Predictive maintenance strategies
- Remote monitoring capabilities
- Advanced variable frequency drive implementations
- Performance optimization for early morning and late afternoon operation

5.6.3 Broader Application Contexts

- Scaling studies across different aquaculture environments

- Comparative analyses with alternative renewable energy configurations
- Long-term performance and reliability assessments
- Development of standardized empirical testing protocols to supplant theoretical PSH calculations

5.7 Concluding Remarks

The research substantiates the potential of integrated floating photovoltaic systems as a sustainable, technically robust solution for aquaculture aeration. This study contributes significantly to advancing renewable energy applications in agricultural technology by demonstrating economic viability and environmental benefits.

The developed system represents a promising pathway toward more sustainable and energy-efficient aquaculture practices, offering a replicable model for transition from conventional fossil fuel-dependent technologies to renewable energy solutions.

5.8 Research Implications

The results elucidate the paramount significance of technological innovation in mitigating environmental issues, especially within agriculture and aquaculture. By adeptly amalgamating renewable energy technologies with operational efficacy, this investigation offers a persuasive framework for the sustainable management of resources.

The research methodology, which emphasizes empirical field validation instead of mere theoretical estimations, sets a noteworthy benchmark for forthcoming studies in renewable energy, thereby underscoring the critical necessity of evaluating real-world performance in the design and execution of systems.

List of Bibliography

[1] Kumar, A., Singh, R., & Patel, D. (2023). Advances in aquaculture aeration systems: A comprehensive review. *Aquacultural Engineering*, 96, 102337.

[2] Liu, Z., Ma, C., Li, X., Deng, Z., & Tian, Z. (2023). Aquatic environment impacts of floating photovoltaic and implications for climate change challenges. *Journal of Environmental Management*, *346*, 118851.

[3] Martinez-Cordero, F. J., Leung, P., & Chen, Y. S. (2021). Compressed air systems in intensive aquaculture: Performance and economic analysis. *Aquaculture Economics & Management*, 25(2), 156-173.

[4] Li, H., Cui, Z., Cui, H., Bai, Y., Yin, Z., & Qu, K. (2023). A review of influencing factors on a recirculating aquaculture system: Environmental conditions, feeding strategies, and disinfection methods. *Journal of The World Aquaculture Society*. https://doi.org/10.1111/jwas.12976

[5] Kumar, A., Patel, S., Yoshida, T., & Menon, R. (2024). Comparative analysis of dissolved oxygen monitoring strategies in solar-powered aquaculture aeration systems: Single-point versus spatial distribution approaches. Aquacultural Engineering, 105(3), 213-229. https://doi.org/10.1016/j.aquaeng.2023.11.005

[6] Zhang, J., Wang, S., & Liu, G. (2022). Comparative analysis of electrochemical and optical dissolved oxygen sensors: Performance and reliability in full-scale

[7] Chai, H., Song, X., Yang, Y., & Liu,J. (2023). Energy-efficient dissolved oxygen control using reinforcement learning in wastewater treatment plants. Water Research, 230, 119503. https://doi.org/10.1016/j.watres.2023.119503

[8] Park, J., Kim, M., & Lee, S. (2022). Deep reinforcement learning for dissolved oxygen control in activated sludge processes. Chemical Engineering Journal, 437, 135318. https://doi.org/10.1016/j.cej.2022.135318

[9] Wu, J., Lin, H., & Zhang, M. (2023). Machine learning-based dissolved oxygen control strategies in wastewater treatment plants: Implementation and energy saving potential. Journal of Cleaner Production, 389, 135797. https://doi.org/ 10.1016/j. jclepro.2023.135797

List of Bibliography (Continued)

[10] Liu, Y., Chen, S., & Wang, Q. (2022). Spatial-temporal analysis of dissolved oxygen distribution in oxidation ditches using wireless sensor networks. Environmental Technology, 43(9), 1289-1301. https://doi.org/10.1080/09593330.2022.2041095

[11] Venkatesh, G., & Elankovan, R. (2023). IoT-based dissolved oxygen monitoring and control system for energy optimization in biological nutrient removal. Environmental Technology & Innovation, 29, 102971. https://doi.org/10.1016/j.eti.2022.102971

[12] Hasan, M., Ahmed, S., & Kumar, P. (2024). Novel anti-fouling coatings for optical dissolved oxygen sensors: Performance evaluation in high-solids astewater environments. Sensors and Actuators B: Chemical, 385, 133814. https://doi.org/10.1016/j.snb.2023.133814

[13] Santoro, D., Bertanza, G., & Lampis, S. (2023). Long-term reliability assessment of optical dissolved oxygen sensors in high-strength industrial wastewater applications. Water Environment Research, 95(4), e12724. https://doi.org/10.1002/wer.12724

[14] Newhart, K.B., Holloway, R.W., & Cath, T.Y. (2022). Data-driven digital twins for process optimization in water resource recovery facilities. Water Research X, 15, 100140. https://doi.org/10.1016/j.wroa.2022.100140

[15] Poch, M., Cortés, U., & Comas, J. (2023). Digital twins for wastewater treatment plants: Current applications and future perspectives. Science of The Total Environment, 858, 159760. https://doi.org/10.1016/j.scitotenv.2022.159760

[16] Wang, X., Li, Y., & Zhou, Q. (2022). Multi-parameter sensors for simultaneous monitoring of dissolved oxygen and nutrients in wastewater treatment: A review. Frontiers of Environmental Science & Engineering, 16(6), 78. https://doi.org/10.1007/s11783-022-1541-9

[17] Zhu, Z., Yang, K., & Chen, Y. (2023). Integrated multiparameter sensor arrays for real-time monitoring of biological nutrient removal processes. ACS Sensors, 8(3), 1027-1039. https://doi.org/10.1021/acssensors.2c02352

List of Bibliography (Continued)

[18] Rosso, D., & Jenkins, D. (2024). Carbon-neutral wastewater treatment: Engineering strategies and operational considerations. Water Science & Technology, 89(1), 1-22. https://doi.org/10.2166/wst.2023.391

[19] Yuan, Z., Marques, R., & Keller, J. (2022). Advances in real-time control for energy-efficient wastewater treatment: A critical review. Water Research, 218, 118452. https://doi.org/10.1016/j.watres.2022.118452

[20] Prateek, J. (2023). Enabling Floating Solar Photovoltaic (FPV) Deployment in Southeast Asia: Overview with Considerations for Aquaculture PV. https://doi.org/10.2172/1957987

[21] Mohammad, B. R., Joessianto, E. P., Annas, S. S., Hendro, A. W., & P., A. (2023). Performance Evaluation Of Floating Solar Power Plant In Sidobandung Bojonegoro. *The Spirit of Society Journal*. https://doi.org/10.29138/scj.v6i2.2197

[22] Zahra, S. G., Ayyad, A., & van Sark, W. (2023). Offshore floating photovoltaics system assessment in worldwide perspective. *Progress in Photovoltaics*. https://doi.org/10.1002/pip.3723

[23] Mucha, S. (2024). A microcontroller-based approach to control oxygen and stablish flexible acclimation regimes. *bioRxiv*. https://doi.org/10.1101/2024.06.03.597140

[24] Tran, Đ. C., Dien, D. N., Nguyen, C. C., & Vu, V. T. (2023). Design and manufacture control system for water quality based on IoT technology for aquaculture in Vietnam. *Bulletin of Electrical Engineering and Informatics*, 12(4). https://doi.org/10.11591/eei.v12i4.5180

[25] Sagnik, Bhattacharya., Anik, Goswami., Pradip, Kumar, Sadhu. (2023). 3. Design, development and performance analysis of FSPV system for powering sustainable energy based mini micro-grid. doi: 10.1007/s00542-023-05457-2

[26] Ann, M., Nardulli. (2023). PV Temperature Prediction Incorporating the Effect of Humidity and Cooling Due to Seawater Flow and Evaporation on Modules Simulating Floating PV Conditions. Energies, doi: 10.3390/en16124756

List of Bibliography (Continued)

[27] Lal, J., Vaishnav, A., Kumar, D., Jana, A., Jayaswal, R., Chakraborty, A., Kumar, S., Devati, Pavankalyan, M., & Sahil. (2024). Emerging Innovations in Aquaculture: Navigating towards Sustainable Solutions. *International Journal of Environment and Climate Change*, 14(7), 4254. https://doi.org/10.9734/ijecc/2024/v14i74254

[28] Koondhar, M. A., Albasha, L., Mahariq, I., Graba, B. B., & Touti, E. (2024). Reviewing floating photovoltaic (FPV) technology for solar energy generation. Energy Strategy Reviews, 54, 101449. https://doi.org/10.1016/j.esr.2024.101449

[29] Zhang, Y., Wang, J., & Li, X. (2022). *Performance analysis of floating photovoltaic systems for aquaculture oxygenation*. International Journal of Hydrogen Energy. https://doi.org/10.1016/j.ijhydene.2022.02.034

[30] Mohammad, B. R., Joessianto, E. P., Annas, S. S., Hendro, A. W., & P., A. (2023). Performance Evaluation Of Floating Solar Power Plant In Sidobandung Bojonegoro. *The Spirit of Society Journal*. https://doi.org/10.29138/scj.v6i2.2197

[31] Exley, G., Page, T., Thackeray, S. J., Folkard, A. M., Couture, R.-M., Hernandez, R. R., Cagle, A. E., Salk, K. R., Clous, L., Whittaker, P., Chipps, M., & Armstrong, A. (2022). Floating solar panels on reservoirs impact phytoplankton populations: A modelling experiment. *Journal of Environmental Management, 324*,16410. https://doi.org/10.1016/j.jenvman.2022.116410

[32] Kjeldstad, T., Lindholm, D., Marstein, E., & Selj, J. (2021). Cooling of floating photovoltaics and the importance of water temperature. *Solar Energy, 218,* 544–551. https://doi.org/10.1016/j.solener.2021.03.022

[33] Zahra, S. G., Ayyad, A., & van Sark, W. (2023). Offshore floating photovoltaics system assessment in worldwide perspective. *Progress in Photovoltaics*. https://doi.org/10.1002/pip.3723

[34] Prateek, J. (2023). Enabling Floating Solar Photovoltaic (FPV) Deployment in Southeast Asia: Overview with Considerations for Aquaculture PV. https://doi.org/10.2172/1957987

List of Bibliography (Continued)

[35] Wang, T., Liu, Y., & Chen, J. (2023). Deep learning applications transforming sustainable aquaculture: A comprehensive review. Reviews in Aquaculture, 15(1), 145-172.

[36] Li, H., Wang, Y., & Zhang, Q. (2022). Early disease detection in farmed salmon using deep convolutional neural networks. Aquacultural Engineering, 98, 102241.

[37] Zhao, J., Wang, Q., & Liu, C. (2024). Real-time pathogen detection in recirculating aquaculture systems using deep learning. Aquaculture, 577, 739982.

[38] Chen, W., Zhang, L., & Wang, X. (2023). Transformer architectures for water quality prediction in recirculating aquaculture systems. Computers and Electronics in Agriculture, 205, 107523

[39] Garcia-Martinez, C., Rodriguez, A., & Smith, T. (2022). Deep neural networks for growth rate forecasting in tilapia farming. Aquaculture, 562, 738756.

[40] Kim, J., & Johnson, L. (2024). Transfer learning approaches for species-specific disease detection in aquaculture. IEEE Transactions on Artificial Intelligence, 5(1), 78-93.

[41] Park, S., Lee, J., & Kim, H. (2022). Adapting pre-trained computer vision models for shrimp health assessment. Aquaculture International, 30(5), 2453-2469.

[42] Santos, M., Oliveira, T., & Costa, B. (2023). Deep reinforcement learning for optimal feeding strategies in sea bass production. Aquaculture Research, 54(2), 763-779.

[43] Zhang, P., Li, W., & Johnson, T. (2024). Reinforcement learning approaches for resource optimization in intensive aquaculture systems. Applied Soft Computing, 146, 110456.

[44] Martínez-Álvarez, F., García, A., & López, J. (2023). Edge computing implementations for real-time aquaculture monitoring and control. Sensors, 23(4), 1789-1805.

[45] Wilson, J., Anderson, K., & Brown, S. (2024). Remote monitoring solutions using edge computing in offshore aquaculture. Journal of Marine Science and Engineering, 12(2), 234-251.

List of Bibliography (Continued)

[46] Ahmed, M., Khan, S., & Johnson, R. (2022). Multimodal deep learning for comprehensive aquaculture monitoring. Aquacultural Engineering, 96(3), 102-118.

[47] Patel, R., & Thompson, M. (2024). Environmental variability and model robustness in aquaculture AI systems. Fish and Fisheries, 25(1), 112-129.

[48] Yu, L., Zhang, C., & Wong, D. (2022). Challenges in developing deep learning solutions for small-scale aquaculture operations. Aquacultural Engineering, 97, 102238.

[49] Battisti, L. (2023). Energy, power, and greenhouse gas emissions for future transition scenarios. *Energy Policy*, *179*, 113626. https://doi.org/10.1016/j.enpol.2023.113626

[50] Zhang, L., Liu, Y., & Wang, H. (2023). Comprehensive assessment of greenhouse gas emissions from integrated aquaculture-solar systems: A life cycle approach. Renewable and Sustainable Energy Reviews, 168, 112828.

[51] Chen, J., Thompson, M., & Anderson, K. (2024). Emission reduction potential of floating photovoltaic systems in aquaculture: A global perspective. Environmental Science & Technology, 58(3), 1642-1653.

[52] Kim, S., & Park, J. (2023). Seasonal variation in greenhouse gas emissions from integrated aquaculture-solar facilities: A case study from Southeast Asia. Aquacultural Engineering, 99, 102355.

[53] Wang, R., Zhang, Q., & Li, X. (2024). Carbon payback analysis of floating solar photovoltaic systems: Methodology and applications in aquaculture. Journal of Cleaner Production, 415, 137582.

[54] IEA. (2023). CO_2 Emissions from Fuel Combustion. International Energy Agency.

[55] United Nations Framework Convention on Climate Change (UNFCCC). (2023.). AM009: Tool to calculate project or leakage CO2 emissions from fossil fuel combustion. Retrieved from http://cdm.unfccc.int/methodologies/ PAmethodologies/ tools/am-tool- 09-v2.0.pdf/history_view

List of Bibliography (Continued)

[56] *Dissolved-oxygen-analyzers*. (n.d.). Solutions/Products-and- Services/Measurement/ Analyzers/Liquid-Analyzers. Retrieved January 1, 2025, from https://www. yokogawa.com/solutions/products-and-services/measurement/analyzers/liquid-analyzers/dissolved-oxygen-analyzers/multi-channel-4-wire-analyzer-flxa402/

[57] Thermal Mass Flow Meter. (2025). Retrieved January 1, 2025, https://cdsentec. com/thermal-mass-flow-meter/

[58] Elprocus. (2025). What is pyranometer: Construction, types & applications. Retrieved January 1, 2025,https://www.elprocus.com/what-is-pyranometer-construction-types-applications/

[59] Yokogawa. (2025). Touch Screen GP10/GP20. Retrieved January 1, 2025, https://www.yokogawa.com/solutions/products-and-services/measurement/ data-acquisition-products/portable-data-acquisition/touch-screen-gp10-gp20/# Details__ Easy-Predictive-Detection

[60] Yokogawa Meters & Instruments. (2025). Press releases. Yokogawa. Retrieved January 1, 2025, https://www.yokogawa.com/news/press-releases/2013/2013-01-09/

[61] Kaya, D., Phelan, P., Chau, D., & Sarac, H. I. (2002). Energy efficiency in compressed air systems. Energy Conversion and Management, 43(16), 2311–2322. https://doi.org/10.1016/S0196-8904(02)00026-8

[62] International Organization for Standardization (ISO). (2009). ISO 1217:2009: Displacement compressors — Acceptance tests. Geneva, Switzerland: ISO.

[63] Compressed Air and Gas Institute (CAGI). (2020). Performance verification of compressed air systems. Retrieved from https://www.cagi.org

[64] Saidur, R., Rahim, N. A., & Hasanuzzaman, M. (2010). A review on compressed-air energy use and energy savings. Renewable and Sustainable Energy Reviews, 14(4), 1135–1153. https://doi.org/10.1016/j.rser.2009.11.013

[65] U.S. Department of Energy (DOE). (2003). Improving compressed air system performance: A sourcebook for industry. Washington, DC: U.S. DOE.

APPENDICES

APPENDICES A

List of Table 1

List of Table 1

Table 1: One-Day Measurement Data of Air Flow, Dissolved Oxygen, Power Input, and Solar Radiation (20 November 2023)

Time	Air Flow(Nm/hr)	DO (mg/l)	Power Inverter (Watt)	Solar Radiation (W./m2)
08:00:00	0.21	3.76	1,105.10	322.29
08:05:00	0.21	3.79	1,105.16	350.31
08:10:00	0.20	3.75	1,105.40	353.47
08:15:00	0.21	3.79	1,105.46	380.71
08:20:00	1.85	3.58	1,297.80	400.81
08:25:00	0.21	3.75	1,105.64	409.66
08:30:00	0.21	3.85	1,105.74	426.69
08:35:00	0.20	3.95	1,105.76	443.09
08:40:00	0.21	3.87	1,105.72	467.38
08:45:00	0.20	3.91	1,105.92	485.09
08:50:00	4.49	3.75	1,509.92	507.06
08:55:00	6.43	3.80	1,492.58	523.32
09:00:00	8.10	3.97	1,414.80	539.81
09:05:00	9.46	3.91	1,516.54	550.39
09:10:00	10.48	3.98	1,694.22	557.86
09:15:00	10.71	4.07	1,597.40	598.74
09:20:00	10.81	3.98	1,509.36	611.15
09:25:00	4.49	4.08	1,105.78	624.81
09:30:00	0.20	3.95	1,105.88	647.39
09:35:00	0.20	4.00	1,105.74	658.62
09:40:00	0.20	4.04	1,196.50	674.01
09:45:00	0.19	4.06	1,105.36	680.45
09:50:00	0.20	4.16	1,105.32	694.33
09:55:00	0.19	4.19	1,105.54	696.66
10:00:00	0.20	4.10	1,105.44	723.47
10:05:00	0.19	4.28	1,105.52	728.38
10:10:00	0.20	4.26	1,105.48	736.83
10:15:00	0.20	4.25	1,105.28	749.25
10:20:00	0.19	4.31	1,105.10	748.76
10:25:00	2.93	4.05	1,303.26	755.53
10:30:00	0.19	4.20	1,105.24	764.87
10:35:00	0.20	4.30	1,105.38	770.63
10:40:00	7.41	4.28	1,358.46	749.86
10:45:00	8.04	4.34	1,385.64	707.96

Table 1: One-Day Measurement Data of Air Flow, Dissolved Oxygen, Power Input, and Solar Radiation (20 November 2023) (Continued)

Time	Air Flow(Nm/hr)	DO (mg/l)	Power Inverter(Watt)	Solar Radiation(W./m2)
10:50:00	6.37	4.34	1,410.42	763.24
10:55:00	6.54	4.45	1,398.20	777.04
11:00:00	6.27	4.37	1,300.84	797.11
11:05:00	6.42	4.51	1,379.78	802.97
11:10:00	6.30	4.51	1,301.10	815.94
11:15:00	6.06	4.49	1,410.78	830.76
11:20:00	6.24	4.65	1,497.98	827.31
11:25:00	9.06	4.56	1,399.30	824.93
11:30:00	8.34	4.59	1,412.28	834.94
11:35:00	6.22	4.57	1,391.48	845.73
11:40:00	6.03	4.65	1,410.92	844.73
11:45:00	6.23	4.61	1,401.22	841.20
11:50:00	6.00	4.70	1,313.72	843.51
11:55:00	6.12	4.71	1,209.10	840.70
12:00:00	6.25	4.77	1,301.36	852.33
12:05:00	9.76	4.68	1,411.44	841.67
12:10:00	10.06	4.65	1,418.46	844.17
12:15:00	12.01	4.73	1,509.94	849.99
12:20:00	11.64	4.77	1,509.38	855.11
12:25:00	12.76	4.94	1,840.34	851.37
12:30:00	13.33	4.91	1,877.24	839.99
12:35:00	13.37	5.04	1,520.26	834.21
12:40:00	12.81	5.09	1,652.86	830.25
12:45:00	13.05	5.10	1,597.32	836.39
12:50:00	12.58	5.05	1,471.74	827.87
12:55:00	13.31	4.86	1,574.84	824.24
13:00:00	13.29	5.02	1,617.20	815.96
13:05:00	13.23	4.85	1,596.82	798.50
13:10:00	12.96	4.91	1,597.50	796.69
13:15:00	12.89	5.14	1,627.72	761.76
13:20:00	13.11	5.24	1,670.68	768.70
13:25:00	13.09	5.17	1,761.64	787.49
13:30:00	12.77	5.11	1,508.46	761.23
13:35:00	12.54	5.37	1,508.40	738.69
13:40:00	12.86	5.26	1,786.00	706.39
13:45:00	12.77	5.25	1,696.56	726.88
13:50:00	12.61	5.12	1,596.08	718.93
13:55:00	13.16	5.32	1,696.22	703.04

Table 1: One-Day Measurement Data of Air Flow, Dissolved Oxygen, Power Input, and Solar Radiation (20 November 2023) (Continued)

Time	Air Flow(Nm/hr)	DO (mg/l)	Power Inverter(Watt)	Solar Radiation(W./m2)
14:00:00	12.51	5.47	1,603.14	689.07
14:05:00	13.06	5.31	1,696.66	684.06
14:10:00	12.47	5.10	1,706.24	657.57
14:15:00	12.50	5.15	1,509.00	646.03
14:20:00	12.65	5.26	1,508.78	643.64
14:25:00	12.58	5.46	1,692.52	621.23
14:35:00	12.46	5.26	1,498.44	586.05
14:40:00	12.43	5.39	1,688.88	558.32
14:45:00	12.69	5.41	1,594.00	569.14
14:50:00	12.33	5.42	1,508.36	556.04
14:55:00	12.24	5.30	1,597.66	531.39
15:00:00	12.27	5.25	1,697.10	517.41
15:05:00	12.13	5.52	1,564.62	502.11
15:10:00	12.29	5.45	1,592.18	488.29
15:15:00	11.92	5.46	1,410.82	460.91
15:20:00	11.69	5.45	1,474.28	416.83
15:25:00	11.87	5.58	1,596.30	423.56
15:30:00	11.66	5.61	1,509.22	402.21
15:35:00	11.21	5.46	1,410.84	381.84
15:40:00	11.44	5.37	1,410.60	357.66
15:45:00	10.63	5.55	1,499.08	336.29
15:50:00	10.19	5.37	1,423.16	315.75
15:55:00	10.68	5.64	1,596.60	308.62
16:00:00	10.71	5.61	1,498.96	289.61
16:05:00	10.35	5.55	1,398.52	273.20

APPENDICES B

List of Table 2

List of Table 2

Table 2: Average Operational Parameters Recorded Over One Month (August 2023)

TIME	Solar Radiation(W./m2)	Power Inverter(W)	Air Flow (Litr/min)	DO(mg/l)
08:00:00	302.57	1,138.63	20.14	1.85
08:05:00	324.57	1,176.44	22.53	1.81
08:10:00	317.41	1,200.80	23.78	1.81
08:15:00	324.63	1,202.20	37.98	1.81
08:20:00	356.74	1,274.90	56.60	1.80
08:25:00	347.75	1,299.36	65.17	1.80
08:30:00	402.13	1,342.73	74.99	1.80
08:35:00	387.90	1,338.85	81.35	1.80
08:40:00	419.91	1,409.66	99.44	1.81
08:45:00	426.09	1,425.07	115.86	1.80
08:50:00	440.92	1,436.87	122.59	1.79
08:55:00	446.46	1,477.05	137.93	1.80
09:00:00	458.41	1,486.43	151.35	1.77
09:05:00	482.13	1,507.53	160.65	1.78
09:10:00	488.92	1,524.78	160.91	1.77
09:15:00	533.69	1,535.55	171.84	1.77
09:20:00	555.81	1,538.40	176.63	1.77
09:25:00	565.03	1,528.77	176.90	1.78
09:30:00	596.44	1,558.68	184.21	1.75
09:35:00	585.31	1,573.09	184.68	1.76
09:40:00	633.82	1,562.99	188.93	1.78
09:45:00	594.90	1,531.16	188.12	1.78
09:50:00	623.91	1,573.15	191.93	1.80
09:55:00	594.99	1,569.61	190.18	1.82
10:00:00	609.34	1,552.78	192.71	1.81
10:05:00	640.03	1,529.99	194.83	1.80
10:10:00	647.59	1,580.00	189.37	1.83
10:15:00	653.54	1,541.66	196.84	1.84
10:20:00	643.21	1,522.59	193.67	1.84
10:25:00	671.85	1,579.25	195.17	1.85
10:30:00	651.63	1,575.25	193.74	1.85
10:35:00	659.64	1,567.35	199.65	1.86
10:40:00	676.08	1,561.79	198.69	1.86
10:45:00	676.01	1,559.87	199.44	1.88
10:50:00	681.61	1,538.76	200.85	1.88
10:55:00	700.55	1,539.17	198.77	1.91

Table 2: Average Operational Parameters Recorded Over One Month (August 2023) (Continued)

TIME	Solar Radiation(W./m2)	Power Inverter(W)	Air Flow (Litr/min)	DO(mg/l)
11:00:00	704.17	1,576.24	199.71	1.91
11:05:00	709.73	1,590.88	200.95	1.91
11:10:00	694.06	1,521.79	200.71	1.92
11:15:00	747.99	1,607.18	202.57	1.93
11:20:00	765.87	1,565.90	196.34	1.95
11:25:00	764.37	1,559.24	197.62	1.94
11:30:00	788.67	1,628.68	220.37	1.96
11:35:00	773.48	1,603.06	210.80	2.00
11:40:00	801.65	1,661.82	212.75	2.01
11:45:00	813.79	1,609.85	213.15	2.04
11:50:00	786.09	1,586.64	211.83	2.02
11:55:00	767.86	1,590.28	206.05	2.03
12:00:00	722.47	1,572.19	200.82	2.05
12:05:00	791.98	1,599.24	212.88	2.07
12:10:00	795.56	1,617.33	206.34	2.03
12:15:00	771.53	1,582.81	206.53	2.05
12:20:00	799.70	1,574.87	214.29	2.07
12:25:00	865.34	1,621.56	218.83	2.09
12:30:00	808.25	1,576.02	208.73	2.08
12:35:00	854.37	1,577.39	212.79	2.13
12:40:00	785.41	1,572.70	204.41	2.11
12:45:00	776.57	1,588.59	207.93	2.14
12:50:00	753.13	1,598.92	206.60	2.15
12:55:00	769.79	1,594.10	211.08	2.16
13:00:00	758.92	1,572.49	198.92	2.18
13:05:00	701.39	1,532.00	203.11	2.18
13:10:00	741.93	1,605.85	202.19	2.18
13:15:00	827.91	1,605.74	207.77	2.17
13:20:00	694.18	1,532.62	202.68	2.20
13:25:00	689.25	1,567.77	194.02	2.21
13:30:00	700.23	1,607.84	202.39	2.24
13:35:00	702.30	1,586.54	198.40	2.25
13:40:00	645.77	1,551.69	200.43	2.26
13:45:00	635.04	1,552.52	192.44	2.28
13:50:00	674.28	1,528.98	191.84	2.25
13:55:00	638.20	1,546.81	188.36	2.26
14:00:00	619.83	1,494.87	195.24	2.26
14:05:00	633.61	1,574.58	184.51	2.28
14:10:00	614.05	1,544.76	193.08	2.28

Table 2: Average Operational Parameters Recorded Over One Month (August 2023) (Continued)

TIME	Solar Radiation(W./m2)	Power Inverter(W)	Air Flow (Litr/min)	DO(mg/l)
14:15:00	633.25	1,545.28	194.09	2.31
14:20:00	626.45	1,536.67	196.75	2.29
14:25:00	522.79	1,487.47	176.62	2.33
14:30:00	520.10	1,484.52	178.41	2.35
14:35:00	578.74	1,520.56	188.58	2.33
14:40:00	494.61	1,491.64	176.87	2.34
14:45:00	544.10	1,491.45	179.88	2.34
14:50:00	507.19	1,470.60	173.91	2.35
14:55:00	498.80	1,481.92	169.69	2.35
15:00:00	469.87	1,497.44	169.09	2.37
15:05:00	439.24	1,502.66	166.07	2.40
15:10:00	439.68	1,459.54	169.61	2.38
15:15:00	426.41	1,450.99	160.99	2.40
15:20:00	489.71	1,451.48	164.98	2.40
15:25:00	486.46	1,473.78	163.78	2.42
15:30:00	419.89	1,437.01	163.47	2.42
15:35:00	404.24	1,441.38	157.61	2.43
15:40:00	392.00	1,433.29	152.12	2.44
15:45:00	356.21	1,430.68	143.20	2.43
15:50:00	321.53	1,400.33	134.02	2.43
15:55:00	313.44	1,356.30	126.16	2.46
16:00:00	278.97	1,340.87	110.28	2.43
16:05:00	315.16	1,392.15	128.43	2.45
16:10:00	253.00	1,323.93	111.31	2.45
16:15:00	258.55	1,336.22	106.38	2.44
16:20:00	239.59	1,342.81	109.58	2.44
16:25:00	238.09	1,312.08	103.91	2.47
16:30:00	234.60	1,340.22	98.77	2.46
16:35:00	232.10	1,298.60	93.58	2.46
16:40:00	214.51	1,272.54	80.88	2.48
16:45:00	180.49	1,230.13	65.46	2.49
16:50:00	154.48	1,190.05	51.14	2.50
16:55:00	154.77	1,186.73	38.51	2.50
17:00:00	134.01	1,159.14	27.66	2.53

APPENDICES C

List of Table 3

List of Table 3

Table 3: Average Operational Parameters Recorded Over One Month (September 2023)

TIME	Solar Radiation (W./m2)	Power Inverter(W)	Air Flow (Litr/min)	DO(mg/l)
08:00:00	230.98	1,127.91	9.77	2.17
08:05:00	250.41	1,146.38	8.94	2.18
08:10:00	280.72	1,131.65	14.01	2.19
08:15:00	294.79	1,148.67	14.16	2.20
08:20:00	305.33	1,160.56	18.04	2.22
08:25:00	324.22	1,165.80	23.32	2.23
08:30:00	369.97	1,257.96	42.12	2.24
08:35:00	384.52	1,258.44	49.33	2.27
08:40:00	426.94	1,243.22	50.30	2.30
08:45:00	430.10	1,268.80	61.08	2.31
08:50:00	422.74	1,328.55	68.18	2.33
08:55:00	437.58	1,380.44	89.91	2.34
09:00:00	471.18	1,385.25	104.75	2.36
09:05:00	468.74	1,475.75	122.63	2.36
09:10:00	475.78	1,498.39	136.13	2.40
09:15:00	483.47	1,494.25	142.27	2.41
09:20:00	526.21	1,507.18	152.83	2.44
09:25:00	515.03	1,525.48	155.79	2.44
09:30:00	546.69	1,508.21	153.59	2.46
09:35:00	576.79	1,522.24	162.93	2.45
09:40:00	554.14	1,514.58	160.20	2.48
09:45:00	541.93	1,500.56	166.15	2.48
09:50:00	578.92	1,546.28	176.82	2.50
09:55:00	599.89	1,544.92	179.67	2.51
10:00:00	642.24	1,577.64	189.09	2.52
10:05:00	665.83	1,556.10	185.56	2.54
10:10:00	626.98	1,541.53	181.26	2.56
10:15:00	618.92	1,558.40	179.86	2.58
10:20:00	645.40	1,530.04	178.63	2.59
10:25:00	577.67	1,500.23	169.51	2.61
10:30:00	617.03	1,528.42	173.34	2.61
10:35:00	608.34	1,538.60	176.09	2.61
10:40:00	664.98	1,571.17	183.81	2.62
10:45:00	655.47	1,591.97	185.26	2.64
10:50:00	689.35	1,552.16	189.11	2.65
10:55:00	692.68	1,570.98	191.27	2.68

Table 3: Average Operational Parameters Recorded Over One Month (September 2023) (Continued)

TIME	Solar Radiation (W./m2)	Power Inverter(W)	Air Flow (Litr/min)	DO(mg/l)
11:00:00	700.65	1,574.15	192.06	2.70
11:05:00	698.39	1,572.14	192.29	2.71
11:10:00	661.21	1,569.42	190.49	2.72
11:15:00	754.66	1,580.14	193.06	2.74
11:20:00	747.53	1,568.51	201.68	2.76
11:25:00	697.48	1,570.75	189.51	2.77
11:30:00	665.15	1,567.32	179.48	2.76
11:35:00	648.17	1,500.41	163.83	2.79
11:40:00	648.05	1,500.45	167.77	2.80
11:45:00	612.22	1,531.47	168.41	2.79
11:50:00	654.47	1,519.19	173.96	2.82
11:55:00	549.56	1,491.98	170.78	2.84
12:00:00	622.41	1,540.73	182.99	2.84
12:05:00	622.55	1,505.78	178.49	2.85
12:10:00	580.01	1,489.22	167.57	2.87
12:15:00	619.93	1,521.19	180.04	2.88
12:20:00	625.93	1,533.83	176.16	2.90
12:25:00	620.44	1,530.67	177.93	2.90
12:30:00	557.00	1,476.82	165.65	2.90
12:35:00	590.34	1,484.42	165.04	2.93
12:40:00	544.10	1,469.90	156.72	2.95
12:45:00	631.19	1,492.48	163.73	2.94
12:50:00	596.57	1,498.58	164.69	2.96
12:55:00	618.62	1,482.62	160.37	2.95
13:00:00	572.69	1,506.09	170.59	2.95
13:05:00	498.05	1,469.61	158.57	2.99
13:10:00	600.45	1,483.72	159.75	3.01
13:15:00	559.75	1,479.32	154.91	3.00
13:20:00	581.22	1,519.13	169.27	3.02
13:25:00	553.13	1,533.56	177.59	3.01
13:30:00	528.15	1,509.09	169.78	3.04
13:35:00	536.55	1,495.53	165.29	3.06
13:40:00	522.31	1,468.63	164.86	3.05
13:45:00	546.87	1,507.23	162.43	3.07
13:50:00	514.54	1,486.18	157.81	3.09
13:55:00	459.34	1,468.45	158.39	3.09
14:00:00	457.28	1,442.32	159.12	3.09
14:05:00	425.46	1,433.53	140.52	3.11

Table 3: Average Operational Parameters Recorded Over One Month (September 2023) (Continued)

TIME	Solar Radiation (W./m2)	Power Inverter(W)	Air Flow (Litr/min)	DO(mg/l)
14:10:00	486.07	1,443.12	155.02	3.11
14:15:00	454.78	1,456.59	157.76	3.13
14:20:00	432.54	1,415.08	142.42	3.13
14:25:00	408.26	1,415.39	136.92	3.14
14:30:00	435.62	1,439.39	143.34	3.14
14:35:00	465.68	1,426.98	139.40	3.15
14:40:00	482.30	1,468.87	160.79	3.17
14:45:00	470.94	1,456.66	145.89	3.19
14:50:00	420.34	1,417.25	139.03	3.19
14:55:00	406.63	1,429.10	138.22	3.19
15:00:00	375.26	1,412.82	131.29	3.20
15:05:00	347.85	1,363.45	115.38	3.19
15:10:00	332.03	1,398.44	121.37	3.17
15:15:00	341.80	1,365.00	116.18	3.19
15:20:00	311.73	1,388.89	113.81	3.23
15:25:00	320.18	1,380.39	121.26	3.21
15:30:00	291.18	1,333.13	103.44	3.22
15:35:00	304.44	1,335.70	108.14	3.23
15:40:00	289.79	1,337.68	101.55	3.24
15:45:00	288.58	1,362.16	109.11	3.25
15:50:00	265.06	1,347.01	106.61	3.24
15:55:00	252.20	1,331.97	102.32	3.26
16:00:00	250.26	1,307.89	99.07	3.24
16:05:00	231.90	1,306.89	87.60	3.25
16:10:00	215.56	1,254.47	74.27	3.24
16:15:00	199.79	1,261.44	69.59	3.25
16:20:00	190.56	1,245.97	73.88	3.26
16:25:00	181.55	1,237.17	65.82	3.26
16:30:00	171.40	1,230.04	54.96	3.28
16:35:00	173.10	1,231.63	47.81	3.26
16:40:00	166.63	1,235.19	52.33	3.27
16:45:00	146.91	1,222.70	47.28	3.28
16:50:00	139.04	1,162.54	35.72	3.29
16:55:00	128.25	1,162.45	26.06	3.28
17:00:00	110.72	1,141.70	20.18	3.27

APPENDICES D

List of Table 4

List of Table 4

Table 4: Average Operational Parameters Recorded Over One Month (Octorber 2023)

TIME	Solar Radiation (W./m2)	Power Inverter(W)	Air Flow (Litr/min)	DO(mg/l)
08:00:00	263.65	1,141.51	45.54	2.84
08:05:00	261.83	1,171.34	50.04	2.86
08:10:00	307.26	1,209.43	66.05	2.91
08:15:00	311.54	1,211.26	71.95	2.94
08:20:00	317.85	1,219.38	80.92	2.94
08:25:00	338.17	1,230.74	102.63	2.96
08:30:00	360.50	1,230.90	86.31	3.01
08:35:00	348.39	1,251.36	90.99	2.95
08:40:00	361.54	1,279.23	87.55	2.99
08:45:00	359.52	1,293.15	104.75	2.99
08:50:00	373.72	1,290.35	104.19	3.00
08:55:00	369.92	1,367.12	114.89	2.97
09:00:00	378.07	1,356.72	141.39	2.91
09:05:00	408.85	1,390.53	165.17	2.96
09:10:00	421.55	1,421.48	177.36	2.87
09:15:00	429.65	1,455.20	188.16	2.89
09:20:00	435.78	1,466.98	177.98	2.94
09:25:00	450.64	1,428.85	185.68	2.95
09:30:00	456.63	1,456.64	186.41	2.98
09:35:00	476.40	1,483.71	194.89	2.98
09:40:00	500.77	1,516.45	189.16	2.97
09:45:00	464.62	1,527.60	187.30	2.97
09:50:00	471.21	1,450.65	177.52	3.02
09:55:00	500.79	1,487.84	180.76	3.01
10:00:00	506.06	1,501.79	179.10	3.06
10:05:00	517.05	1,514.47	178.79	3.08
10:10:00	551.51	1,524.27	185.34	3.11
10:15:00	568.72	1,523.98	191.10	3.13
10:20:00	572.71	1,568.95	206.26	3.17
10:25:00	558.49	1,557.94	198.33	3.18
10:30:00	605.46	1,559.51	207.58	3.20
10:35:00	580.57	1,538.05	214.98	3.19
10:40:00	613.74	1,588.11	208.20	3.25
10:45:00	607.52	1,529.64	202.87	3.28
10:50:00	569.44	1,493.43	191.11	3.28
10:55:00	627.29	1,570.91	201.00	3.31

Table 4: Average Operational Parameters Recorded Over One Month (Octorber 2023) (Continued)

TIME	Solar Radiation (W./m2)	Power Inverter(W)	Air Flow (Litr/min)	DO(mg/l)
11:00:00	612.01	1,541.40	198.36	3.34
11:05:00	577.87	1,492.44	189.89	3.36
11:10:00	587.00	1,509.61	180.27	3.37
11:15:00	578.32	1,495.71	184.54	3.39
11:20:00	595.59	1,494.79	187.77	3.41
11:25:00	638.71	1,495.62	181.95	3.47
11:30:00	646.04	1,487.91	183.89	3.54
11:35:00	594.58	1,504.09	186.59	3.52
11:40:00	608.99	1,501.82	194.61	3.57
11:45:00	614.05	1,513.02	188.82	3.54
11:50:00	603.46	1,495.39	189.77	3.54
11:55:00	649.99	1,563.70	202.23	3.56
12:00:00	593.08	1,531.94	200.55	3.59
12:05:00	681.55	1,555.80	202.75	3.62
12:10:00	651.70	1,560.69	200.05	3.60
12:15:00	607.47	1,516.23	199.31	3.65
12:20:00	611.93	1,471.59	190.19	3.69
12:25:00	606.50	1,505.10	188.77	3.71
12:30:00	553.59	1,458.37	176.05	3.76
12:35:00	561.31	1,498.09	184.41	3.77
12:40:00	590.93	1,501.57	192.81	3.80
12:45:00	574.67	1,523.03	189.15	3.76
12:50:00	601.14	1,530.08	191.39	3.79
12:55:00	635.15	1,536.26	201.78	3.83
13:00:00	580.26	1,511.14	187.13	3.81
13:05:00	561.14	1,531.97	193.55	3.85
13:10:00	563.19	1,516.48	190.94	3.90
13:15:00	551.42	1,502.48	193.83	3.91
13:20:00	574.85	1,508.75	205.28	3.93
13:25:00	551.47	1,473.95	193.70	3.91
13:30:00	533.66	1,420.96	172.11	3.90
13:35:00	542.62	1,473.08	177.01	3.94
13:40:00	507.99	1,500.15	178.99	3.95
13:45:00	495.48	1,450.91	173.65	3.97
13:50:00	504.26	1,471.81	175.11	3.95
13:55:00	494.58	1,491.58	178.78	4.02
14:00:00	491.77	1,457.80	177.71	3.99
14:05:00	447.65	1,471.12	141.50	4.04
14:10:00	517.85	1,469.26	150.30	4.04

Table 4: Average Operational Parameters Recorded Over One Month (Octorber 2023) (Continued)

TIME	Solar Radiation (W./m2)	Power Inverter(W)	Air Flow (Litr/min)	DO(mg/l)
14:15:00	459.67	1,441.41	155.66	4.08
14:20:00	457.77	1,476.53	140.78	4.07
14:25:00	453.79	1,479.29	138.36	4.07
14:30:00	432.77	1,450.69	113.43	4.06
14:35:00	448.14	1,431.93	129.35	4.09
14:40:00	386.34	1,426.16	97.56	4.06
14:45:00	398.71	1,403.22	133.21	4.06
14:50:00	373.49	1,388.64	109.02	4.07
14:55:00	369.87	1,424.74	136.08	4.07
15:00:00	381.44	1,429.96	132.51	4.12
15:05:00	351.76	1,451.98	138.71	4.11
15:10:00	349.30	1,440.13	132.90	4.14
15:15:00	336.31	1,394.11	130.26	4.20
15:20:00	334.93	1,407.38	136.97	4.21
15:25:00	347.84	1,441.41	146.96	4.12
15:30:00	325.63	1,432.71	143.56	4.16
15:35:00	311.06	1,373.25	148.93	4.21
15:40:00	284.52	1,368.81	139.45	4.24
15:45:00	284.65	1,381.48	124.25	4.20
15:50:00	283.64	1,366.03	143.05	4.19
15:55:00	266.61	1,345.99	135.32	4.17
16:00:00	243.56	1,337.66	136.31	4.15
16:05:00	226.85	1,320.03	120.92	4.17
16:10:00	220.40	1,303.93	134.54	4.31
16:15:00	212.54	1,314.33	149.53	4.28
16:20:00	197.30	1,297.94	103.15	4.24
16:25:00	181.37	1,273.61	87.84	4.30
16:30:00	168.82	1,265.33	66.56	4.34
16:35:00	149.93	1,243.09	35.55	4.30
16:40:00	128.76	1,225.26	24.54	4.24
16:45:00	103.35	1,214.99	70.61	4.34
16:50:00	87.03	1,192.29	64.31	4.40
16:55:00	78.40	1,152.98	57.69	4.43
17:00:00	72.33	1,133.46	51.42	4.47

APPENDICES E

List of Table 5

List of Table 5

Table 5: Average Operational Parameters Recorded Over One Month (Novemberr 2023)

TIME	Solar Radiation (W./m2)	Power Inverter(W)	Air Flow (Litr/min)	DO(mg/l)
08:00:00	265.89	1,175.21	31.07	3.55
08:05:00	293.70	1,187.43	38.24	3.62
08:10:00	316.21	1,217.42	49.48	3.63
08:15:00	320.32	1,235.39	60.75	3.64
08:20:00	339.49	1,227.92	61.67	3.68
08:25:00	356.07	1,269.23	74.13	3.62
08:30:00	388.07	1,284.85	80.14	3.69
08:35:00	406.17	1,313.58	88.40	3.67
08:40:00	424.27	1,319.09	96.37	3.75
08:45:00	431.95	1,333.89	107.43	3.80
08:50:00	465.87	1,392.31	119.94	3.77
08:55:00	471.39	1,446.76	145.44	3.77
09:00:00	498.42	1,519.13	169.24	3.77
09:05:00	509.36	1,537.33	179.48	3.79
09:10:00	528.41	1,572.52	195.94	3.81
09:15:00	558.62	1,565.39	206.43	3.84
09:20:00	572.15	1,485.47	188.53	3.82
09:25:00	565.78	1,471.22	170.73	3.84
09:30:00	581.94	1,421.28	152.77	3.93
09:35:00	598.73	1,412.07	159.92	3.89
09:40:00	605.52	1,434.50	156.93	3.92
09:45:00	585.50	1,417.55	160.92	3.96
09:50:00	624.05	1,437.30	167.56	4.03
09:55:00	639.42	1,434.68	167.38	4.02
10:00:00	635.63	1,462.68	166.68	4.03
10:05:00	654.70	1,460.88	174.02	4.07
10:10:00	648.21	1,454.32	175.04	4.11
10:15:00	688.51	1,470.66	179.88	4.16
10:20:00	694.64	1,453.18	177.24	4.18
10:25:00	669.79	1,457.04	179.97	4.18
10:30:00	718.91	1,481.21	182.52	4.24
10:35:00	674.36	1,457.79	172.26	4.23
10:40:00	693.00	1,467.63	182.32	4.27
10:45:00	695.54	1,483.64	193.67	4.26
10:50:00	695.94	1,486.33	190.51	4.29
10:55:00	673.50	1,469.65	185.21	4.33

Table 5: Average Operational Parameters Recorded Over One Month (Novemberr 2023) (Continued)

TIME	Solar Radiation (W./m2)	Power Inverter(W)	Air Flow (Litr/min)	DO(mg/l)
11:00:00	643.02	1,472.47	180.42	4.30
11:05:00	671.07	1,451.11	175.51	4.33
11:10:00	693.02	1,459.22	175.49	4.32
11:15:00	673.31	1,507.44	195.51	4.34
11:20:00	709.46	1,511.85	191.36	4.40
11:25:00	727.69	1,504.21	194.76	4.41
11:30:00	736.69	1,525.63	195.64	4.45
11:35:00	709.71	1,511.63	198.32	4.47
11:40:00	704.67	1,495.58	194.91	4.49
11:45:00	738.33	1,513.21	200.62	4.51
11:50:00	738.32	1,511.51	205.18	4.55
11:55:00	709.27	1,489.76	199.33	4.53
12:00:00	740.22	1,495.20	208.51	4.60
12:05:00	759.71	1,543.28	214.71	4.61
12:10:00	718.35	1,530.36	213.01	4.62
12:15:00	688.29	1,558.58	220.14	4.68
12:20:00	703.07	1,545.21	224.82	4.69
12:25:00	722.14	1,629.12	220.48	4.71
12:30:00	669.92	1,574.36	215.19	4.75
12:35:00	677.15	1,601.00	226.12	4.76
12:40:00	712.16	1,625.11	233.17	4.79
12:45:00	673.85	1,585.35	230.04	4.78
12:50:00	706.29	1,616.11	231.99	4.81
12:55:00	712.70	1,586.89	236.21	4.83
13:00:00	708.60	1,605.02	239.55	4.80
13:05:00	694.03	1,607.99	228.79	4.81
13:10:00	688.42	1,639.32	230.97	4.84
13:15:00	729.70	1,611.87	241.48	4.89
13:20:00	690.82	1,588.87	227.19	4.92
13:25:00	683.06	1,574.79	220.29	4.91
13:30:00	651.70	1,568.62	224.55	4.95
13:35:00	624.07	1,578.18	224.13	4.98
13:40:00	664.65	1,631.43	231.34	4.93
13:45:00	631.88	1,584.88	228.41	5.01
13:50:00	561.22	1,572.16	210.67	5.02
13:55:00	629.25	1,582.07	214.63	5.15
14:00:00	584.49	1,547.21	199.92	5.19
14:05:00	601.24	1,563.80	214.33	5.20
14:10:00	575.10	1,560.50	206.31	5.07

Table 5: Average Operational Parameters Recorded Over One Month (Novemberr 2023) (Continued)

TIME	Solar Radiation (W./m2)	Power Inverter(W)	Air Flow (Litr/min)	DO(mg/l)
14:15:00	575.65	1,550.24	216.85	5.08
14:20:00	552.06	1,546.67	222.22	5.14
14:25:00	493.16	1,542.69	211.87	5.15
11:20:00	709.46	1,511.85	191.36	4.40
11:25:00	727.69	1,504.21	194.76	4.41
11:30:00	736.69	1,525.63	195.64	4.45
11:35:00	709.71	1,511.63	198.32	4.47
14:30:00	466.25	1,533.85	200.01	5.14
14:35:00	458.61	1,479.23	194.40	5.14
14:40:00	459.27	1,463.32	179.59	5.21
14:45:00	470.14	1,482.08	179.85	5.21
14:50:00	446.01	1,513.15	196.55	5.19
14:55:00	438.07	1,497.36	190.00	5.21
15:00:00	441.03	1,464.97	185.86	5.23
15:05:00	404.01	1,500.36	183.91	5.24
15:10:00	407.71	1,486.44	185.69	5.23
15:15:00	389.83	1,454.94	182.10	5.25
15:20:00	371.89	1,422.92	166.19	5.28
15:25:00	370.45	1,433.50	170.52	5.25
15:30:00	333.26	1,416.86	163.04	5.35
15:35:00	308.73	1,436.43	158.45	5.34
15:40:00	295.24	1,408.63	155.31	5.32
15:45:00	281.88	1,387.07	151.49	5.36
15:50:00	257.64	1,392.91	142.71	5.35
15:55:00	241.13	1,346.79	137.53	5.39
16:00:00	226.55	1,353.29	125.82	5.41
16:05:00	207.93	1,316.40	106.22	5.41
16:10:00	188.16	1,290.09	93.12	5.37
16:15:00	178.46	1,274.23	85.40	5.41
16:20:00	164.17	1,244.16	69.98	5.35
16:25:00	160.30	1,289.12	77.96	5.41
16:30:00	126.30	1,245.94	68.34	5.36
16:35:00	86.75	1,212.65	57.88	5.41
16:40:00	69.07	1,168.51	36.45	5.44

Biography

Name – Surname	Mr. Sirisak Pangvuthivanich
Date of Birth	13 March 1974
Address	109/214 Chuanchuen Greenbound Village, Moo.8 Bangkuwat Subdistrict Muangpathumthani District, Pathumthani Thailand 12000
Education	Bachelor Degree in Electrical Engineering, Rajamangala Institute of Technology Krungthep Master of Business Administration, Pathumthani University
Work Experiences	Managing Director at Energy Creation Co., Ltd
Telephone Number	+669-4571-6868
Email Address	Sirisak_p@mail.rmutt.ac.th